J.C. de Veij Mestdagh

The effect of perturbation properties on system identification of human balance control during stance

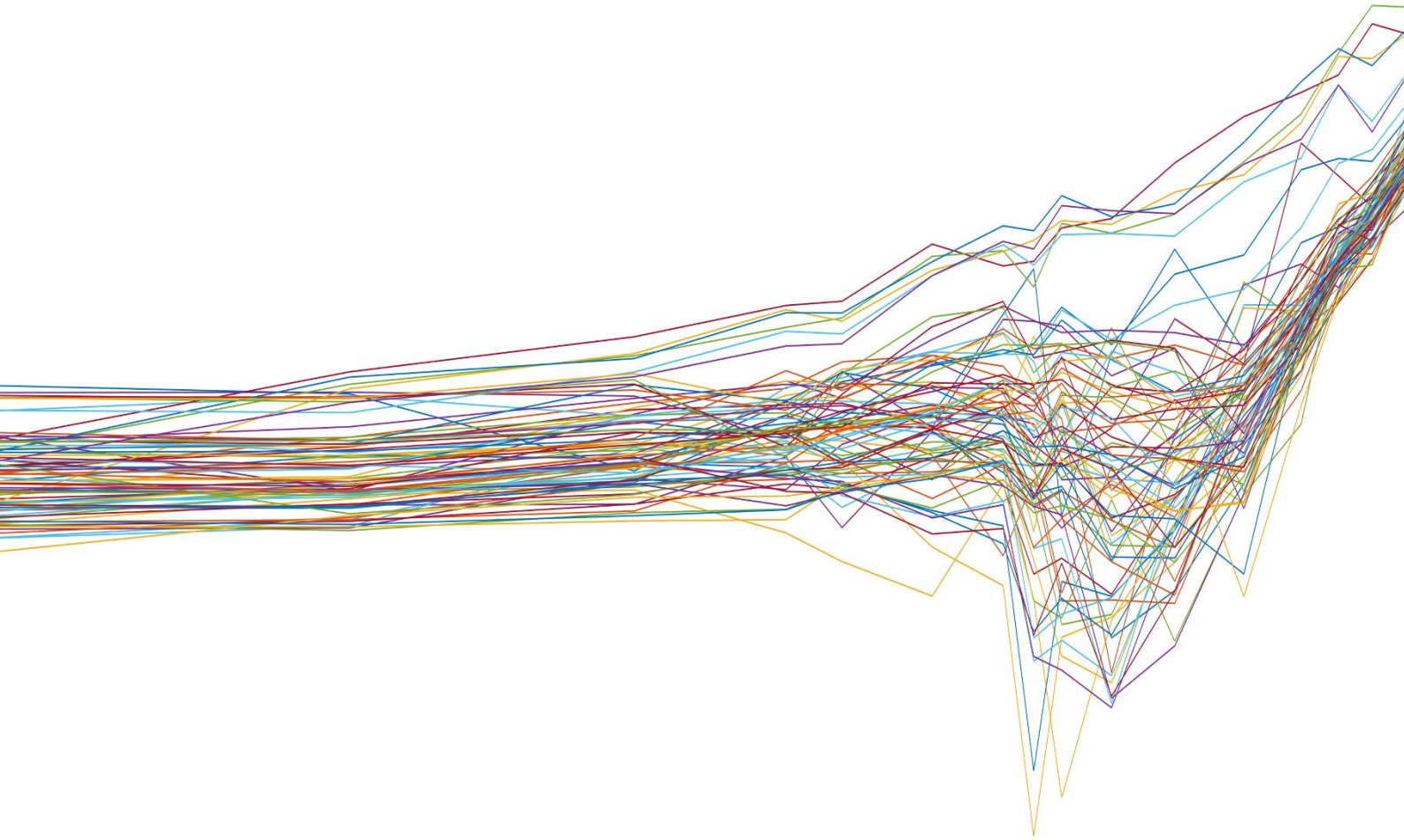

TU Delft

The effect of perturbation properties on system identification of human balance control during stance

by

J.C. de Veij Mestdagh

in partial fulfilment of the requirements for the degree of

Master of Science

in Biomedical Engineering

at Delft University of Technology,

to be defended publicly on Tuesday October 17th at 12:30.

Thesis committee:	dr. ir. A.C. Schouten	TU Delft
	dr. ir. J.H. Pasma,	TU Delft
	ir. I.M. Schut,	TU Delft
	prof. dr. ir. W.A. Serdijn	TU Delft

TU Delft

The effect of perturbation properties on system identification of human balance control during stance

Jurriaan C. de Veij Mestdagh

ABSTRACT- *Introduction:* System identification of the neuromuscular controller that regulates human balance, gives insight in the causes and effects of human balance disorders. The combination of varying perturbation properties in literature and lack of rationale behind chosen perturbation properties, reveals possible violations of assumptions made to perform system identification. This study investigates the effect of number of repetitions of the perturbation signal and the perturbation amplitude on the identification quality. *Methods:* 12 subjects were perturbed at their support surface with a multisine signal. Kinematics of the subjects were recorded with a motion capture system; ground reaction forces were recorded with force plates. The best linear approximation of the neuromuscular controller was identified. Measures for variability of identification with respect to the number of repetitions and for nonlinearity with respect to the perturbation amplitude were calculated. *Results:* Identification variability was found to significantly decrease with number of repetitions. Nonlinearity within the neuromuscular controller increased significantly with perturbation amplitude. *Conclusions:* After having measured 6-8 repetitions, measuring subsequent repetitions does not decrease identification variability significantly for the following 6-7 repetitions. The balance between suppressing noise effects by using a high amplitude perturbation and minimising nonlinear effects by using a low amplitude perturbation was identified to be optimized between a perturbation signal amplitude of 8 cm PtP and 11 cm PtP.

INTRODUCTION

Active control is necessary for the inherently unstable human body to maintain an upright posture in the gravitational field. The human body is controlled by the central nervous system (CNS) to counteract the pull of gravity and external disturbances, such as moving support surfaces (for example while standing in a moving bus) or forces on the body (for example force exerted by the wind). To do so, the CNS uses visual, vestibular and proprioceptive sensory feedback to gain information about the current posture of the body. Using this information, the CNS invokes balance recovering corrective torques by activating muscles around the ankle, knee and hip joints.

Ageing, medication side-effects, and pathologies such as stroke, Parkinson's disease, and cerebral palsy can affect human balance control resulting in balance disorders[1–3]. As balance control consists of an interplay between sensory cues, control in the CNS and muscle actions, the source of a balance disorder is hard to determine. To treat patients with balance disorders with personalized and targeted interventions, it is therefore important to know what subsystem of human balance control is affected and in which manner.

From an engineering perspective, the human balance system can be considered a closed loop system. Following this approach, we model the human body as an inverted pendulum, acting as the plant P (Figure 1). The plant is controlled by the neuromuscular controller (NMC), representing the CNS. The NMC receives feedback about the state of the pendulum, which for a SIP, is the rotation around the SIP's joint axis.

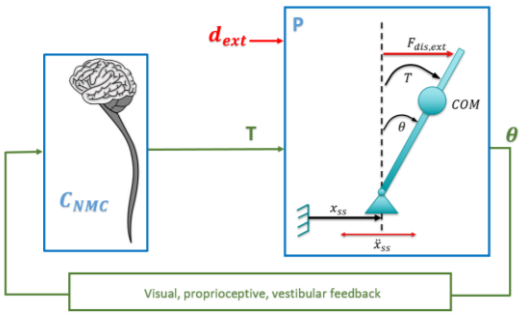

Figure 1: Human balance control scheme. The human body, plant P, is modelled as an inverted pendulum, challenged in upright position by external perturbation d_{ext}, either presented as an external force $F_{dis,ext}$ or a support surface translation $\ddot{x}_{ss}$. Information about the state of the body (θ) is fed back into the neuromuscular controller C_{NMC}, which outputs a corrective ankle torque T.

Because the human balance system is a (closed loop) feedback system, causes and effects are interrelated. To gain more insight in the underlying mechanisms and distinguish cause and effect, closed loop system identification (SI) techniques can be applied[4]. In system identification, a system is perturbed to gain information about its behaviour. SI is used in various papers[5–8] to investigate balance pathologies by identifying the controller of the human balance system, called the neuromuscular controller (NMC).

Noise, introduced into the loop by internal noises of the human and measurement noise, influences the results of SI. Therefore, in most SI applications, noise is decreased by averaging over multiple repetitions of the same perturbation. The result of identification of the NMC is therefore dependent on the amount of repetitions which is averaged over.

Furthermore, single-input single-output (SISO) SI needs the assumption of a single inverted pendulum (SIP). However, when perturbation amplitude increases, the human changes from a strategy in which the ankles are used to stabilize the body ('ankle strategy'), to a strategy in which the hip joints and possibly the knee joints also contribute to stability ('mixed strategy')[9–11]. When the knee and hip joints are also mobile, the SIP assumption is invalid and the estimation of the NMC (which is only informative on the ankle strategy in SISO SI) might be degenerated. More complex multi-input multi-output SI should be applied in the case of SIP assumption invalidity.

Moreover, the SI method used to identify the NMC assume a linear, time-invariant (LTI) system[12,13]. However, balance control is known to be nonlinear[14] and nonstationary[15]. Nonlinear systems may be approximated by linearization, which is only reasonable within a limited range around the linearization's operating point. When the system is operating too far away from the operating point, for example resulting from a high amplitude perturbation, the accuracy of the linearization diminishes.

Additionally, the NMC might change its behaviour within the ankle strategy with increasing perturbation amplitude. This could result in a different identification of the NMC in different perturbation amplitude conditions.

These effects indicate that the assumptions made to be able to apply SI on the human balance system, might be violated when the number of repetitions and the perturbation amplitude are chosen arbitrarily.

From literature on human balance system identification[4–8,16–30], no general conclusions can be drawn on which perturbation signal properties are optimal for SI of the NMC, because the authors do not mention the rationale behind the used perturbation signal properties, such as the number of repetitions or the perturbation amplitude. Furthermore, the signal properties differ significantly between studies. For example, the number of repetitions varies between 3 to 16 repetitions and support surface translations differ from 0.5 cm to 23 cm in studies where the NMC is estimated[4–8,16–30]. The variation in perturbation signal properties, combined with the lack of mentioned rationale, implies that the some of the used perturbation signals might break assumptions that are made to be able to apply the SI methods, such as the assumption of a linear system.

Therefore, this study will investigate the effect of number of repetitions of the perturbation signal and perturbation amplitude on the identification of the NMC in healthy adults.

We hypothesize that increasing the number of repetitions available to estimate the NMC, will decrease the variability of the identification result, by reducing the influence of disturbing noises through averaging.

Furthermore, we hypothesize that decreasing perturbation amplitude will decrease the signal-to-noise ratio and therefore decrease the identification accuracy. On the other hand, increasing the perturbation amplitude, might increase nonlinearity of the NMC in two different ways:

1) the NMC will start to operate outside of the range in which it can be considered linear, from here on called "type I nonlinearity"
2) the NMC will change behaviour within the ankle strategy, i.e. change to a different operating point, from here on called "type II nonlinearity"

Lastly, we hypothesize that the assumption of a single inverted pendulum (SIP) will be increasingly violated when perturbing subjects with a higher perturbation amplitude, e.g. by shifting balance strategy from mainly using the ankle joints for stability to the mixed use of the ankles, hips and knees for balance control[31].

The results of this study will contribute to the selection of appropriate perturbation signal properties for SI application in human balance control, reducing noise and nonlinearity contributions that can decrease the quality of the identification result.

METHODS

A. Participants

Twelve healthy subjects (six women; median age 26 years, range 24-65 years, length 1.73 m ± 0.09 m) participated in the study. This study was approved by the Human Research Ethics Committee of Delft University of Technology. All subjects gave written informed consent before participating in the study.

B. Apparatus and Recording

Experiments were performed using the GRAIL system (MotekForce Link, Amsterdam, the Netherlands). GRAIL consists of a split belt treadmill with 6 degrees of freedom force plates beneath the belts, surrounded by ten motion capture cameras (Vicon Bonita, Vicon

Motion Systems, Oxford, UK) and a semi-cylindrical screen (Figure 2).

The positions of motion capture markers were recorded in the Vicon Nexus 2.5 software with a sampling frequency of 100 Hz. Force information from the instrumented treadmills was recorded at 1000 Hz using the D-Flow software that drives GRAIL and streamed to Vicon Nexus, which saved both motion capture data and force plate data.

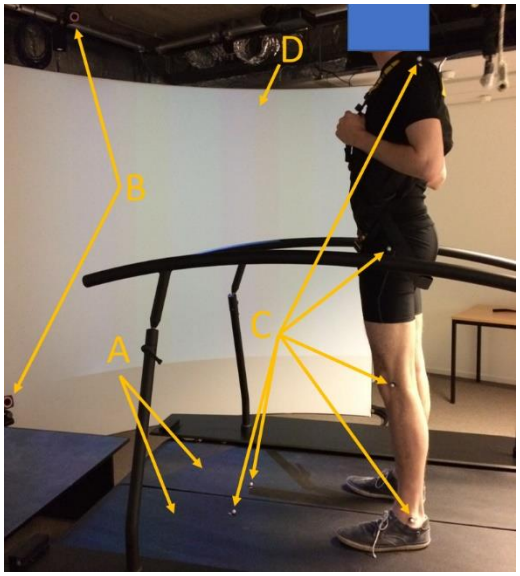

Figure 2: GRAIL system with dual belt instrumented treadmill (A), motion capture cameras (B), subject, motion capture markers (C) and semi-cylindrical screen (D).

C. Perturbation Signal

Both treadmill belt positions were controlled using the same multisine signal. A multisine is a signal composed of the superposition of sines with various frequencies and various amplitudes:

$$d_{ext,in}(t) = \sum_{k=1}^{N} A_k(2\pi f_o kt + \phi_k)$$

where:

- $d_{ext,in}(t)$ is the perturbation signal as input to the GRAIL system
- k is the frequency line, an integer number which corresponds to the Fourier coefficients.
- A_k is the amplitude at frequency line k, which can be zero or nonzero. The frequencies where amplitude A_k is nonzero, are called the excited frequencies f_{ex}.
- f_0 is the frequency resolution ($f_0 = 1/T$ where T is the period of the signal).
- ϕ_k is a random phase at frequency line k.
- N is the number of samples in one period of the signal.
- t is the time vector.

The perturbation signal used in this study was designed to excite specific frequencies, which are distributed logarithmically between 0.05 Hz and 5 Hz on odd frequency lines (k=1, 3, 7, 11, 13, 17, 21, 23, 25, 29, 35, 43, 51, 57, 63, 75, 91, 99). The remaining, nonexcited frequencies, enable analysis of nonlinear contributions[32], see *Data Analysis*.

The designed perturbation signal has a flat velocity spectrum (Figure 3), except for the first excited frequency ($f_0 = 0.05\ Hz$), for which the amplitude was decreased, such that it was, in position spectrum, equal to the magnitude of the second excited frequency ($f_1 = 0.15\ Hz$). The perturbation signal lasts for 20 s. The same phase realisation of the perturbation signal was used for all experiments. The amplitude of the perturbation signal varies between conditions (see 'Conditions').

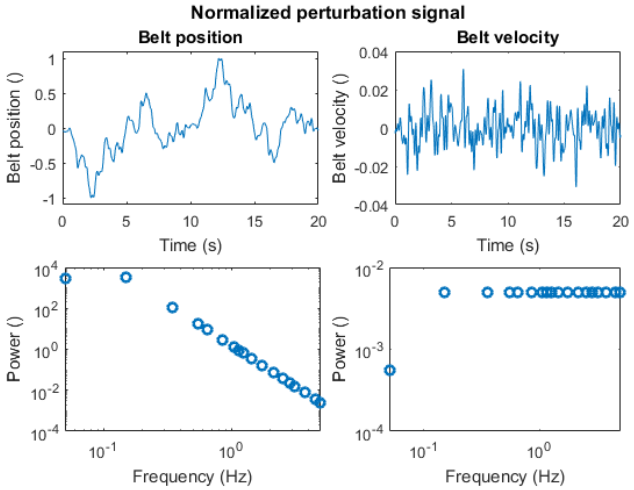

Figure 3: Normalized time signal (top), and the corresponding power spectrum (bottom) for the position (left) and corresponding velocity (right) perturbation signal of the treadmill belt.

D. Conditions

To study the effect of perturbation amplitude, seven distinct amplitude conditions were created by scaling of the perturbation signal. The perturbation amplitudes ranged from 0.02 m peak to peak (PtP) in the A2 condition to 0.2 m PtP in the A20 condition, as shown in Table 1.

Table 1: Experimental conditions.

Condition	m PtP	# trials	# repetitions total	# repetitions for analysis
A2	0.02	1	6.5	6
A5	0.05	1	6.5	6
A8	0.08	4	26	24
A11	0.11	1	6.5	6
A14	0.14	1	6.5	6
A17	0.17	1	6.5	6
A20	0.20	1	6.5	6
Total		**10**		

Each amplitude condition was presented in a separate trial, containing 6.5 repetitions of the scaled perturbation signal, resulting in trials of 130 s. Of every recorded trial, the first 0.5 repetition was discarded to eliminate transient effects, resulting in 6 repetitions available for analysis, which is a moderate value compared to literature[4–8,16–30].

The trial containing the A8 condition, which uses a moderate perturbation amplitude compared to literature[4–8,16–30], was repeated four times, resulting in 24 repetitions available for analysis of the effect of number of repetitions. All other trials were presented once to each subject, resulting in a total amount of 10 trials being presented to each subject (Table 1).

E. Procedure

Reflective motion capture markers were symmetrically attached to the subjects on the following body landmarks: acromioclavicular joints (shoulders), major trochanters (hips), lateral epicondyles (knees) and lateral malleoli (ankles). Furthermore, a marker was attached on each treadmill belt (Figure 2).

Subjects were asked to stand on the treadmill with eyes open and arms crossed over the chest. Subjects were secured using a body harness to prevent falling, which did not constrain movement. The semi-cylindrical screen displayed a grey environment with two static horizontal white lines for visual reference.

First a static trial was recorded, which required the subjects to stand upright comfortably for five seconds. After that, the subjects practiced during three trials of one minute, of which no data were recorded, in which they were perturbed with A2, A11 and A20 perturbations. After practicing, all 10 full-length (130 s) trials were presented in a random order and data were recorded. Between each trial (including practice trials), the subjects could take an optional break of one minute.

F. Data Analysis

1) Pre-processing

Marker data and force plate data were analysed in MATLAB R2016b (MathWorks, Natick, MA, USA). Force plate data were resampled to 100 Hz to match the marker data sample frequency.

2) External Perturbation, Body Sway, and Ankle Torque Signal, Discrete Fourier Transforms and Power Spectral Densities

The external perturbation signal $d_{ext}(t)$ was recorded using markers on the treadmill belts.

To calculate angular displacement of the inverted pendulum over time, i.e. body sway $u_{bs}(t)$, the centres of mass (CoM) of body segments and of the total body were calculated according to Winter et al. (1990)[33] from the marker data of each perturbation trial. Furthermore, the length of the inverted pendulum was calculated from static trial marker data and was defined as the length from the body CoM to the ankle joint in the sagittal plane. The body CoM position in perturbation trials and the length of the inverted pendulum from the static trial were then used to calculate $u_{bs}(t)$ per perturbation trial, which was defined as the angle between body CoM in the sagittal plane and the line perpendicular to the floor plane.

To calculate the ankle torque $y_{tor}(t)$ per perturbation trial, the dynamic centre of pressure (CoP) was calculated from the force plate data. $y_{tor}(t)$ was then determined by calculating the torque that the forces at the CoP exert around the ankle joint axis, as $y_{tor}(t) = F_z(t) * CoP(t) + F_y(t) * h_{ankle}(t)$, in which $F_y(t)$ and $F_z(t)$ are the normal and friction force on the treadmill belt in the sagittal plane and $h_{ankle}(t)$ is the height of the ankle, determined from marker data.

All signals $(d_{ext}(t), u_{bs}(t), y_{tor}(t))$ were divided into the 6.5 repetitions that were recorded for each condition and the first 0.5 repetition was discarded to eliminate transient effects. For each of the remaining six repetitions in $d_{ext}(t), u_{bs}(t)$, and $y_{tor}(t)$, the single sided Discrete Fourier Transform (DFT) was calculated, resulting in $U_{bs}(f), Y_{tor}(f)$ and $D_{ext}(f)$.

Power spectral densities were calculated according:

$$PSD_x = \frac{1}{N}|X(f)|^2$$

where PSD_x is the power spectral density of $x(t)$, N the total number of samples in the signal, and $X(f)$ the DFT of $x(t)$.

3) Frequency Response Functions & Coherence

The frequency response function $C_{NMC}(f)$ of the NMC can be defined as:

$$C_{NMC}(f) = C_{BLA}(f) + C_{SNL}(f) + C_{noise}(f)$$

in which $C_{BLA}(f)$ is the best linear approximation (BLA) of the system, $C_{SNL}(f)$ represents stochastic nonlinear distortions, and $G_{noise}(f)$ represents distortions of the BLA estimate due to the presence of noise. C_{noise} is assumed to be zero-mean noise, uncorrelated to the perturbation signal. G_{SNL} is constant over repetitions

when a constant (single phase realisation) perturbation signal is used.

The BLA of the NMC's FRF was estimated on the excited frequencies with an open loop estimator, by dividing the average Discrete Fourier Transform (DFT) of the sway signal by the average DFT of the torque signal at the excited frequencies[34]:

$$C_{BLA}(f) = \frac{\overline{Y_{tor}}(f_{ex})}{\overline{U_{bs}}(f_{ex})}$$

where $\overline{U_{bs}}(f)$ and $\overline{Y_{tor}}(f)$ are the mean DFT of $u_{bs}(t)$ and $y_{tor}(t)$ over repetitions respectively and f_{ex} represents the excited frequencies.

Furthermore, the coherence functions between the external perturbation signal and the body sway signal $\gamma^2_{d_{ext}u_{bs}}(f)$, and between the external perturbation signal and the ankle torque signal $\gamma^2_{d_{ext}y_{tor}}(f)$ were calculated on the excited frequencies, according:

$$\gamma^2_{xy}(f) = \frac{\left|\overline{S_{xy}}(f_{ex})\right|^2}{\overline{S_{yy}}(f_{ex})\overline{S_{xx}}(f_{ex})}$$

where $\overline{S_{xy}}$ represents the mean cross-spectral density (CSD) of x with y over repetitions and $\overline{S_{xx}}$ is the mean autospectral density (ASD) of x over repetitions. Mean CSDs and ASDs were estimated by multiplying the single sided DFTs with conjugates and averaging over repetitions:

$$\overline{S_{xy}} = \frac{1}{R}\sum_{r=1}^{R} X(f) * Y^*(f)$$

where R is the number of repetitions.

4) Analysing Identification Variability with Respect to Number of Repetitions

The influence of the number of repetitions was examined by using the 24 repetitions that were recorded for the A8 condition. To do so, for every number of repetitions, 15 combinations of that number of repetitions were randomly drawn from the available 24 recorded repetitions. So, for one repetition, one repetition was drawn 15 times; for two repetitions, a random combination of two repetitions was drawn 15 times, etc. For 24 repetitions, only one combination was possible, so this amount of repetitions was not included in the analysis.

For every drawn combination, the BLA was estimated, resulting in 15 BLA estimations per amount of repetitions. The standard deviation between the 15 BLAs was calculated for each number of repetitions, which served as a measure for variability:

$$m^{[x\ reps]}_{variability}(f) = \sqrt{\frac{\sum_{\mathrm{i}=1}^{\mathrm{N}}\left(C^{[x,i]}_{BLA}(f) - \overline{C^{[x]}_{BLA}(f)}\right)^2}{\mathrm{N}-1}}$$

where:

- $m^{[x\ reps]}_{variability}(f)$ is a measure of identification variability when x repetitions are used for identification.
- $C^{[x,i]}_{BLA}(f)$ is the best linear approximation of the controller calculated with the ith combination of x repetitions.
- $\overline{C^{[x]}_{BLA}(f)}$ is the mean BLA over all combinations for this amount of repetitions
- N is the number of combinations drawn for each number of repetitions (i.e. 15).

A higher value for $m^{[x\ reps]}_{variability}$ means more variability in identification of the NMC, a lower value means a steadier identification.

5) Quantifying Type I Nonlinearity

While a linear system only generates output at the excited frequencies, type I nonlinear contributions show up at the nonexcited frequencies as well. Furthermore, noise appears in all frequencies, resulting in the following distribution of contributions:

- At the (odd) excited frequencies: linear + odd nonlinear + noise contributions
- At the even (nonexcited) frequencies: even nonlinear + noise contributions
- At the odd nonexcited frequencies: odd nonlinear + noise contributions

Because of the distribution of contributions, it is possible to quantify nonlinear distortions on the FRF by observing the level of distortions at the nonexcited frequencies[35].

First, the output spectrum was corrected for possible inaccuracy caused by the GRAIL system, for example due to inaccurate perturbation signal tracking. A first order correction was applied, as described in Schoukens et al. (2001)[36]:

$$\tilde{Y}_{tor}(f) = Y_{tor}(f) - \tilde{C}_{BLA}(f)U_{bs}(f)$$

where

- $\tilde{Y}_{tor}(f)$ is the corrected output spectrum.
- $\tilde{C}_{BLA}(f)$ is the BLA interpolated to the nonexcited frequencies.

By interpolating the level of distortions of the corrected output spectrum at the nonexcited frequencies to the excited frequencies and dividing by the spectrum of the input at the excited frequencies, an estimation of the total distortion of the BLA, σ_{total} was obtained[36]. Furthermore, the noise standard deviation σ_{noise} was estimated by calculating the standard deviation of the mean BLA at the excited frequencies.

Next, an estimate of the contribution of the stochastic nonlinear distortions to the bias of the BLA was obtained by:

$$\sigma_{NL}(f) = \sqrt{\left|\sigma_{total}^2 - \sigma_{noise}^2\right|}$$

where σ_{noise} is the noise standard deviation and σ_{total} is the total standard deviation. Due to interpolation problems at the first, second and last excited frequency, σ_{total} and σ_{NL} were only available at 15 of the 18 excited frequencies.

To know the relative influence of the stochastic nonlinear distortions, a measure for type I nonlinearity was defined as the ratio between the standard deviation due to stochastic NL distortions and standard deviation of the noise on the mean BLA, calculated over P consecutive periods. The type I nonlinearity measure was calculated at the frequencies on which both σ_{NL} and σ_{noise} exist:

$$m_{NL1}(f) = \frac{\sigma_{NL}(f_{ex,exist})}{\sigma_{noise}(f_{ex.exist})}$$

where

- $m_{NL1}(f)$ is a measure for type I nonlinearity.
- $f_{ex,exist}$ represents the exited frequencies at which both exist, which are all excited frequencies except the 1st, 2nd, and last excited frequency, due to interpolation issues at both ends of the frequency range.

The measure m_{NL1} represents the relative amount of type I nonlinearity in the system. The higher the ratio (m_{NL1}), the more type I nonlinear behaviour of the NMC.

6) Quantifying Type II Nonlinearity

Type II nonlinearity was defined as the change of control behaviour of the NMC within the ankle strategy. Therefore, type II nonlinearity was expected to be observed as a change of the identified BLA FRF when a different perturbation amplitude is applied.

Accordingly, a measure of type II nonlinearity was defined by:

$$m_{NL2}^{[amp\ x]}(f) = \left|\left|C_{BLA}^{[amp\ x]}(f)\right| - \left|\overline{C_{BLA}^{[all\ amps]}}(f)\right|\right|$$

where

- $m_{NL2}^{[amp\ x]}(f)$ is the measure for type II nonlinearity for perturbation amplitude x.
- $C_{BLA}^{[amp\ x]}(f)$ is the BLA estimate for perturbation amplitude x.
- $\overline{C_{BLA}^{[all\ amps]}}(f)$ is the mean BLA estimate over all perturbation amplitudes.

The measure $m_{NL2}^{[amp\ x]}(f)$ represents the amount a BLA estimate calculated at a specific perturbation amplitude differs from the average BLA estimate over all perturbation amplitudes, therefore a higher value of $m_{NL2}^{[amp\ x]}(f)$ indicates higher type II nonlinearity.

7) Single Inverted Pendulum (In)validity

The assumption of a single inverted pendulum was checked by observing the ankle, knee and hip joint angles. These joint angles were calculated by computing the angle between segments in the sagittal plane, as shown in Figure 4.

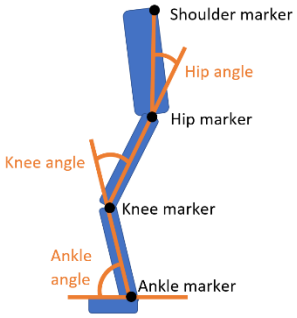

Figure 4: Joint angle definitions in the sagittal plane

Two measures for single inverted pendulum invalidity were calculated as the ratio between PSD's of the knee and ankle angle and the hip and ankle angle:

$$m_{xIP,ka}(f) = \frac{PSD_{knee}(f_{ex})}{PSD_{ankle}(f_{ex})}$$

$$m_{xIP,ha}(f) = \frac{PSD_{hip}(f_{ex})}{PSD_{ankle}(f_{ex})}$$

where

- $m_{xIP,ka}(f)$ and $m_{xIP,ha}(f)$ are measures for single inverted pendulum invalidity.
- $PSD_x(f)$ is the power spectral density of the specified joint angle.
- f_{ex} are the excited frequencies.

When the measures $m_{xIP,ka}(f)$ and $m_{xIP2,ha}(f)$ are significantly larger than one, the knee and hip joints are more affected by the perturbation than the ankle joint angle, rendering the SIP assumption less valid. Therefore, $m_{xIP,ka}(f)$ and $m_{xIP2,ha}(f)$ represent the invalidity of the single inverted pendulum assumption.

8) Frequency Groups & Averaging Measures over Frequencies and Subjects

All five measures ($m_{variability}(f)$, $m_{NL1}(f)$, $m_{NL2}(f)$ $m_{xIP,ka}(f)$, and $m_{xIP,ha}(f)$) are a function of frequency. For further analysis, all measures were split into three frequency groups: low, medium and high. Each group contained 6 excited frequencies (Table 2).

Table 2: Frequency groups

Low	Medium	High
Frequencies in each frequency group (Hz)		
0.05	1.05	2.55
0.15	1.15	2.85
0.35	1.25	3.15
0.55	1.45	3.75
0.65	1.75	4.55
0.85	2.15	4.95

To yield a single value per measure per frequency group, the measures were averaged over the frequencies within the frequency group.

Calculation of mean FRFs over subjects was done by averaging the complex numbers of the FRF over all subjects. Mean coherences and mean measure values over subjects was done by first calculating the measure per subject, and then averaging over subjects.

9) Statistical analysis

For all five measures ($m_{variability}, m_{NL1}, m_{NL2}, m_{xIP,ka}$, and $m_{xIP,ha}$), a two-way repeated measures ANOVA was performed to analyse whether the number of repetitions or the perturbation amplitude had a significant effect on each measure, and to investigate whether the effects were different for each frequency group. An effect was considered significant when the p-value fell under 0.05.

If interaction was significant, for each frequency group a post-hoc one-way repeated measures ANOVA was performed. Bonferroni corrections were applied to the p-values of these three separate tests, to counteract the problem of false-positives when doing multiple comparisons. The Bonferroni correction amounted to a multiplication of the p-values by three, because for each of the three frequency groups, a post-hoc test was done.

RESULTS

All subjects were able to complete all trials without moving their feet (stepping out). Figure 5 gives an overview of the perturbation signal tracking by the treadmill belts for the two extreme perturbation amplitude conditions (A2 and A20).

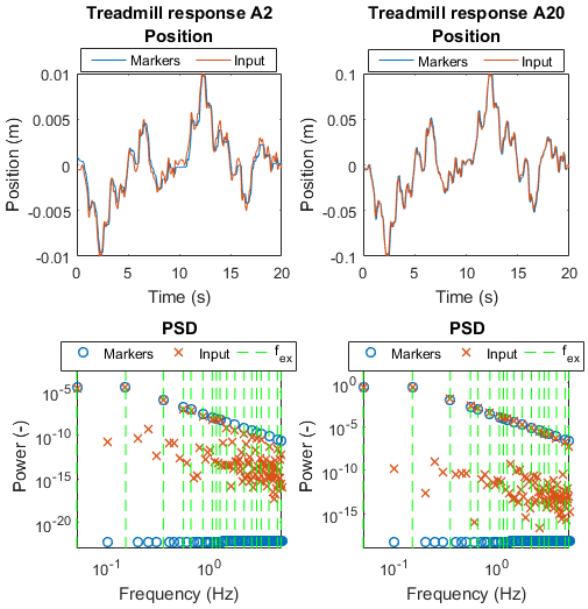

Figure 5: Perturbation signal tracking by treadmill belts for A2 condition (left) and A20 condition (right), position (top) and power spectral density (bottom).

Perturbation signal tracking was better for higher perturbation amplitudes. In general, perturbation tracking was good.

A. Body Sway, Ankle Torque, FRF

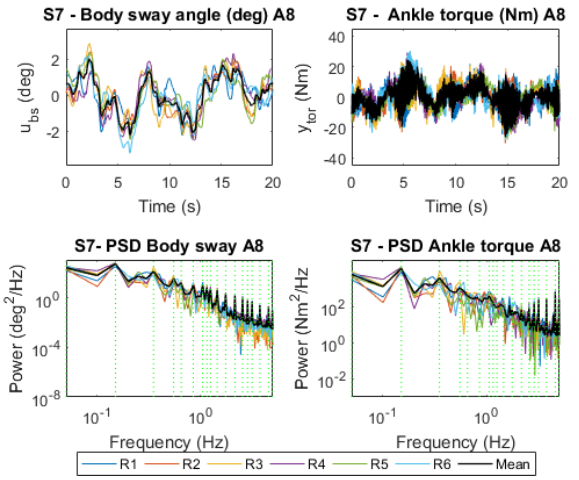

Figure 6: Body sway (left) and ankle torque (right) signals (top), with corresponding power spectral densities (bottom). Six repetitions and the mean over repetitions are shown.

In Figure 6, the body sway angle and ankle torque signals with corresponding power spectral densities are shown for one representative subject in the A8 condition. All six repetitions and their mean are shown.

In both power spectral densities, the peaks at the excited frequencies are easily recognizable.

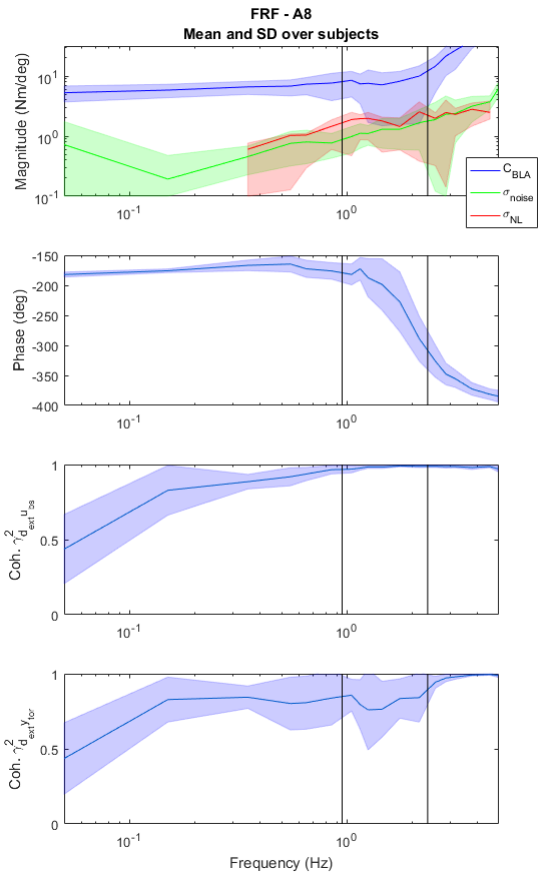

Figure 7: Mean and standard deviation of FRF magnitude with σ_{NL} and σ_{noise} (top), FRF phase (second panel), coherence from external perturbation to body sway (third panel) and coherence from external perturbation to ankle torque (bottom), averaged over subjects. The low, medium and high frequency groups are divided by a solid black line.

The mean and standard deviation over FRFs for all subjects in the A8 condition are shown in Figure 7. Both the coherence from external perturbation to body sway and from external perturbation to torque are plotted. Furthermore, σ_{NL} and σ_{noise} are plotted.

B. Effect of Number of Repetitions

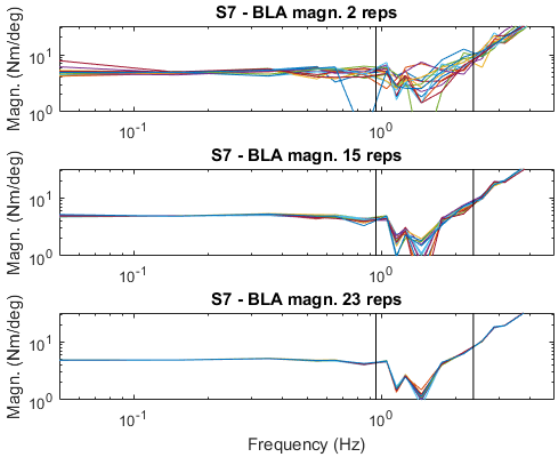

Figure 8: BLA magnitude plots for a representative subject. Every subplot contains 15 BLAs (for 15 samples). The low, medium and high frequencies are divided by a solid black line.

In Figure 8, BLAs calculated from all 15 samples are plotted for various numbers of repetitions for a representative subject. Less variability in identification is obtained when using more repetitions.

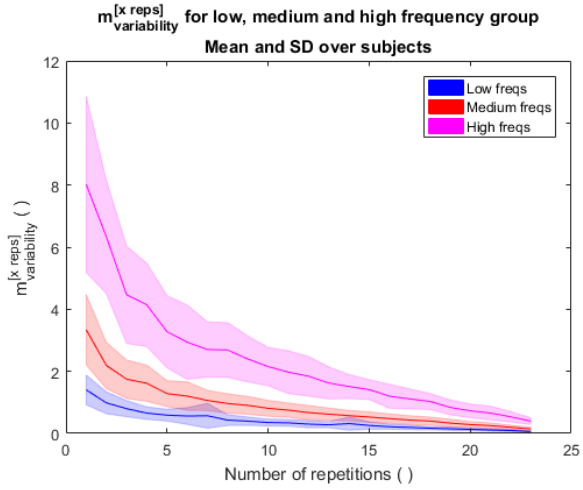

Figure 9: Mean and standard deviation of $m_{variability}^{[x\ reps]}$ for all numbers of repetitions, averaged over subjects.

Figure 9 shows $m_{variability}^{[x\ reps]}$ for all numbers of repetitions for which there were samples. The two-way repeated measures ANOVA revealed a significant interaction effect.

Post hoc tests revealed significant decreases in variability with number of repetitions for the low, medium and high frequency group ($p < 0.001$ for all frequency groups).

C. Effect of the Perturbation Amplitude

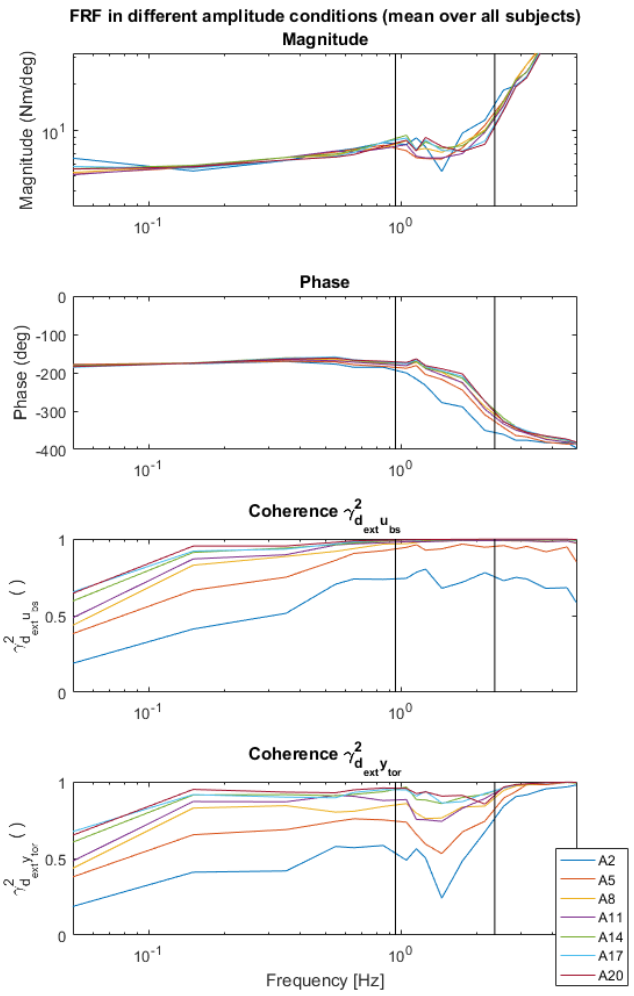

Figure 10: Mean of FRF magnitude (top), FRF phase (second panel), coherence from external perturbation to body sway (third panel) and coherence from external perturbation to ankle torque (bottom) for each perturbation amplitude condition, averaged over subjects. The low, medium and high frequency groups are divided by a solid black line.

FRF's averaged over all subjects for different perturbation amplitudes are shown in Figure 10. The coherences from external perturbation to body sway and to torque are shown. It can be clearly seen that for lower perturbation amplitudes (A2 and A5), coherences are lower.

1) Type I Nonlinearity

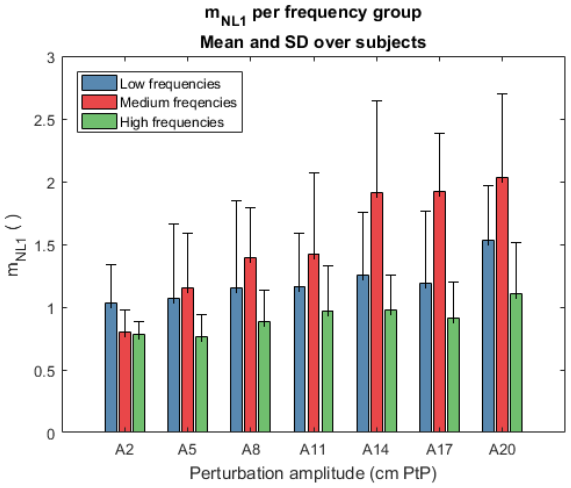

Figure 11: Mean and standard deviation of m_{NL1} for different perturbation amplitudes and frequency groups, averaged over subjects.

In Figure 7 (and Figure 17 in the Appendix) mean FRF plots with σ_{noise} and σ_{total} can be found. Figure 11 shows, for each perturbation amplitude, the mean and standard deviation of the nonlinearity measure for type I nonlinearity (m_{NL1}) for each frequency group, averaged over all subjects.

The two-way repeated measures ANOVA showed there was a significant interaction between the effects of perturbation amplitude and frequency group ($p < 0.001$). Post hoc analysis showed that within the low and high frequency groups, there was no significant effect of perturbation amplitude ($p = 0.537$ and $p = 0.060$ respectively), whereas in the medium frequency group, the measure for type I nonlinearity significantly increases with perturbation amplitude ($p < 0.001$).

2) Type II Nonlinearity

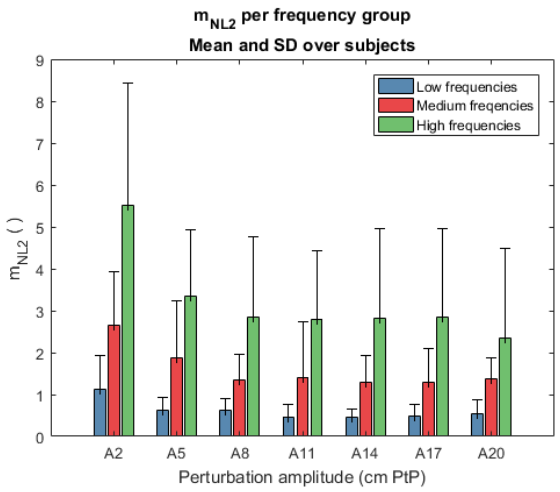

Figure 12: Mean and standard deviation of m_{NL2} for different perturbation amplitudes and frequency groups, averaged over subjects

Figure 12 shows, for each perturbation amplitude, the mean and standard deviation of the nonlinearity measure for type II nonlinearity (m_{NL2}) for each frequency group, averaged over all subjects. The two-way repeated measures ANOVA showed a significant interaction effect of perturbation amplitude and frequency group on the measure for type II nonlinearity ($p = 0.001$).

Post hoc analysis revealed a significant decrease of type II nonlinearity with perturbation amplitude for all frequency groups ($p = 0.024$, $p = 0.009$ and $p = 0.009$, respectively).

3) SIP Invalidity

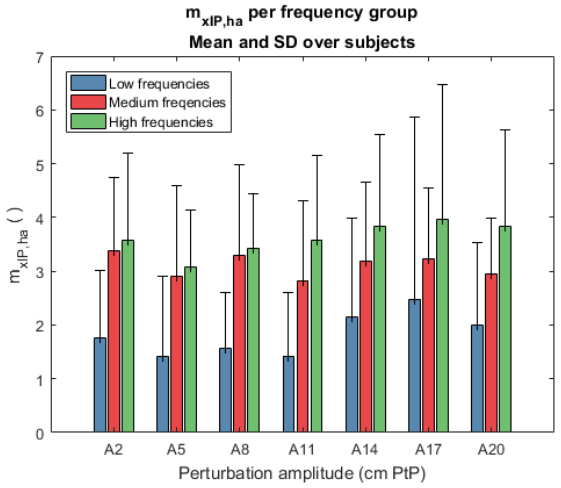

Figure 13: Mean and standard deviation of $m_{xIP,ha}$ for different perturbation amplitudes and frequency groups, averaged over subjects.

Figure 13 shows the measure for SIP invalidity related to the hip joint angle. The two-way repeated measures ANOVA showed no significant effect of perturbation amplitude or interaction effects on SIP validity ($p = 0.289$ and $p = 0.774$ respectively).

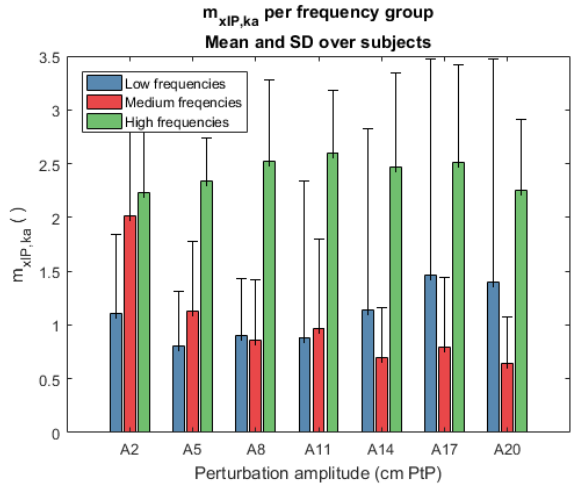

Figure 14: Mean and standard deviation of $m_{xIP,ka}$ for different perturbation amplitudes and frequency groups, averaged over subjects.

Figure 14 shows the SIP invalidity related to the knees, $m_{xIP,ka}$. The two-way repeated measures ANOVA revealed a significant interaction effect.

Post hoc analysis showed that $m_{xIP,ka}$ was not significantly influenced by the perturbation amplitude in the low and high frequency groups ($p = 1.000$ and $p = 1.000$ respectively), but it decreased significantly with perturbation amplitude in the medium frequency group ($p < 0.001$).

DISCUSSION

By perturbing subjects standing upright on a treadmill and recording the ankle torque and body sway, we were able to construct the BLA for the NMC for each subject. By constructing a measure for identification variability and three measures of NMC nonlinearity, the variability of the BLA identification with respect to the number of repetitions that are used for identification and the nonlinearity of the NMC with respect to the perturbation amplitude was investigated.

A. Effect of the number of repetitions

We hypothesized that an increasing number of repetitions would decrease variability in identification. As the results show, the variance of the identification result over samples indeed significantly decreases with the number of repetitions for all three frequency groups. This indicates that adding more repetitions increases the identification consistency.

However, recording more repetitions costs time. Therefore, researchers want to strike a balance between number of repetitions and the influence of noise on the identification result. As can be seen in Table 4, Table 5, and Table 6 in the Appendix, pairwise comparisons show that some numbers repetitions are followed by numbers of repetitions that do not differ significantly in the measure of variability. For example, when having measured 6 repetitions, additionally measuring the 7th, 8th, 9th 10th, 11th and 12th repetition does not decrease the variability of identification for high frequencies significantly. Table 7 in the Appendix shows the mean number of insignificantly differing subsequent repetitions for all numbers of repetitions, over all frequency groups. There is a peak around 6-8 repetitions. In other words, when having measured 6-8 repetitions, the variability does not decrease significantly for the most subsequent repetitions compared to other numbers of repetitions.

B. Effect of the Perturbation Amplitude

For all subjects, the perturbation amplitude ranged from a barely noticeable perturbation amplitude of 2 cm PtP to a perturbation amplitude of 20 cm PtP. In this paragraph, we will discuss the effect of the perturbation amplitude on the body sway and torque signal, and on both nonlinearity measures discussed previously.

1) Perturbator System Linearity & Coherence

The response of the treadmill was inspected to ensure correct tracking of the perturbation signal. For low amplitude perturbation signals, noise is of a greater influence on the tracking than for large amplitude perturbation signals. This can be seen in Figure 5, in which the time series and the auto spectral densities of the input signal are compared to those of the resulting treadmill belt movement. The figure further shows that in the perturbation signal as executed by the treadmill, energy is already transferred from the excited frequencies to the nonexcited frequencies. This means that the generator of the perturbation, in our case the GRAIL system, is behaving nonlinearly itself. Therefore, we cannot assume that all power in nonexcited frequencies in the body sway and ankle torque signals (Figure 3) comes from NMC nonlinearity, because the GRAIL is injecting energy at the nonexcited frequencies into the loop. The amount of energy in the excited frequencies in the perturbation signal is shown in Table 3 in the Appendix. This is compensated for using the perturbator system impurity correction, see *Frequency Response Functions & Coherence*.

Despite some perturbator system nonlinearity, the excited frequencies contain more power than the nonexcited frequencies, as shown by the peaks in the power spectral density plots in Figure 3. This means that exciting specific frequencies by perturbing a subject standing on treadmill belts with a multisine with these specific frequencies, transfers to the body sway and ankle torque signals. In other words, the perturbation signal and the body sway and torque signal are somewhat coherent. This is also seen in Figure 10, which furthermore shows that the coherences from external perturbation to body sway and from external perturbation to ankle torque increase with perturbation amplitude. This is an expected result, as the increase in perturbation amplitude suppresses the effect of noises present in the human balance system and in recording systems (motion capture and force plates) and therefore increases coherence.

2) Effect on Type I Nonlinearity

We hypothesized that type I nonlinearity would increase with perturbation amplitude. The measure for type I nonlinearity is based on analysis of the power that a nonlinear system transfers from excited frequencies to nonexcited frequencies. By applying the analysis as described in Schoukens et al. (2001)[36], the contributions of noise and stochastic nonlinearities to the standard deviation of the identified BLA were separated.

The results showed that the measure for type I nonlinearity in the NMC, m_{NL1}, indeed increases with perturbation amplitude, but only significantly for the medium frequency group. The increase in this type of nonlinearity shows that by increasing perturbation amplitude, the NMC is pushed further away from its linearization operating point and therefore the control system cannot be approximated by a linear system anymore. This effect is also visible in the body sway signals in the time domain, which can be found in the Appendix, where for all subjects, the body sway range increases with perturbation amplitude.

Qualitatively inspecting the medium frequency bars in Figure 11, there seems to be larger increase in m_{NL1} between A11 and A14 than between other perturbation amplitudes. Furthermore, the interaction effect is an interesting result: type I nonlinearity only increases significantly with perturbation amplitude in the medium frequency group. Qualitatively looking at Figure 11, we see that the measure also slightly increases in the other frequency groups.

3) Effect on Type II Nonlinearity

We hypothesised that as perturbation amplitude increases, the balance system would change balance operation, which would be visible as a different shape of the identified BLA's FRF. Therefore, the measure for type II nonlinearity was based on the difference between the identified BLA for a specific perturbation amplitude and the mean BLA over all perturbation amplitudes.

The results show an effect that is opposing expectations: for all three frequency groups, the measure for type II nonlinearity significantly decreases with perturbation amplitude. The difference can be explained by the results found for coherence values and by looking at the total standard deviations of the FRFs, plotted in Figure 15. As the perturbation amplitude increases, noise effects are suppressed. The identification at the A2 condition especially is

influenced by noise. At perturbation amplitudes larger than A5, the measure for m_{NL2} stabilizes.

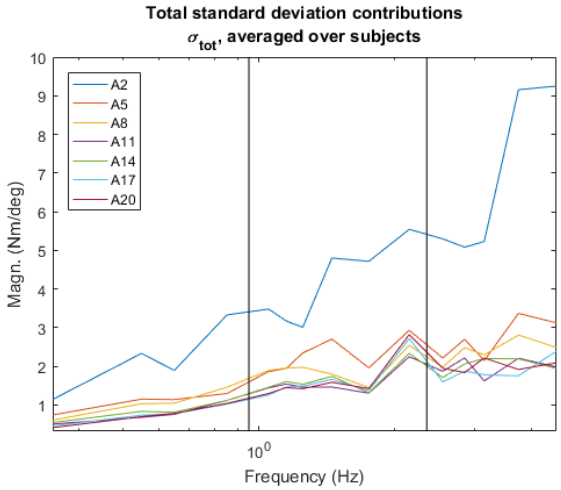

Figure 15: Mean total standard deviation contributions (σ_{total}) for BLAs, averaged over subjects (note: linear scale in y).

This effect indicates that m_{NL} is not the best measure for changing balance operation, as it is more influenced by noise and type I nonlinearity (the two contributions to σ_{total}) than by balance operation changes.

4) Effect on SIP Validity

We hypothesized that increasing the perturbation amplitude would generate knee and hip joint angle rotations that render the SIP assumption invalid.

The two measures for SIP invalidity, $m_{xIP,ka}$ and $m_{xIP,ha}$, are based on the idea that when the transfer function from external perturbation to a joint angle is large, this joint angle is heavily influenced by the external perturbation. By dividing the transfer functions of knee and hip joint angles by the ankle joint angle, we compare the amount of joint angle rotations in the hip and the knee to the rotations in the ankle joint.

Of course, the measures for SIP invalidity do not describe any active contributions, as they are not related to joint torques but to joint angles. The measures are therefore only informative on the SIP assumption and not informative on joint control. Furthermore, an ankle joint angle displacement of 1 degree has a larger influence on the position of the CoM of the human body than a displacement of 1 degree of the knee angle or a displacement of 1 degree of the hip joint angle, because of its position in the 3-link inverted pendulum arising from 3 mobile joints. Therefore, it is no surprise that the values for $m_{xIP,ha}$ and $m_{xIP,ka}$ are steadily larger than 1: this does not mean that the knee and hip joint influence on the CoM's position is larger than that of the ankle. In other words: values larger than one do not immediately invalidate the SIP assumption.

No significant effect of the perturbation amplitude on the measure for SIP invalidity related to the hips was found. This means that, contrary to our expectations and literature[9–11,37], in this study, the hips show no increasing contribution to the stability of the human when the perturbation amplitude increases. However, when qualitatively looking at Figure 13, a slight increase in the measure might be seen. This could indicate that the effect is there, but the statistical power of measuring 12 people is not enough to result in a significant effect.

Furthermore, results show no significant trend in perturbation amplitude dependency of the measure of SIP invalidity related to the knees, for the low and high frequency group. Even more surprisingly, for the medium frequency group, $m_{xIP,ka}$ decreases significantly with perturbation amplitude, contrary to expectation. The trend is especially visible between the A2 and A5 conditions. It seems that the knee joints are more mobile than the ankles at the smallest perturbation amplitudes and medium frequencies, where at higher amplitudes and medium frequencies, the knees are as mobile as the ankles, i.e., the ankles absorb more of the medium frequency perturbations as the perturbation amplitude increases.

5) Finding the Optimal Perturbation Amplitude

The combination of the increase in type I nonlinearity with perturbation amplitude and the low robustness of the identification against noise effects at low perturbation amplitudes shows that there is a balance between noise effects at low perturbation amplitudes and nonlinear effects at large perturbation amplitudes. Godfrey et al. (2005)[38] summarizes this balance as follows:

"For linear system identification, there are two main requirements of a perturbation signal. Firstly, it should be small enough to minimise any nonlinear distortion, and secondly it should be large enough to minimise any noise effects. These requirements are conflicting [..]."

As there is a larger increase in nonlinearity between A11 and A14, and a stabilisation of identification variability due to noise at perturbations larger than A5, we can identify the range of perturbation amplitudes at which this balance is optimized as the range between A8 and A11.

C. Effect of Frequency Groups

As all measures were calculated for the three different frequency groups, an effect of frequency group is visible as well. As this can be informative for researchers searching for information on the effect of frequency on identification variability, nonlinearity and balance strategy, the frequency effects are discussed here.

Firstly, the variability of the identification increases with the frequency group, as seen in Figure 9. This means that the frequency spectrum a researcher is most interested in can also influence the choice for number of repetitions. If the researcher is only interested in identification in the low frequency group, a lower amount of repetitions gives an equal consistency of estimation compared to when the researcher is interested in the higher frequencies as well.

Secondly, an increase of type II nonlinearity with frequency group for all perturbation amplitudes can be seen in Figure 12. As discussed before, this is an indication of an influence of noise, type I nonlinearity or the combination of both, that is increasing with frequency group.

Furthermore, a clear increase in SIP validity related to the hips can be seen in Figure 13. This confirms findings in literature that describe the effect that for slower and low frequency perturbations, the ankle strategy is mostly used, whereas a mixed ankle/hip strategy is used when perturbation speed and/or frequency increase[9–11,37].

Lastly, the measure for SIP validity related to the knees clearly increases strongly with frequency group. Especially the high frequency group shows use of the knees for balance recovery. In most studies, only an ankle strategy and mixed ankle/hip strategy was discussed, however, this result shows that a mixed hip/knee/ankle strategy might exist for high frequency perturbations, which was also reported in Ko (2013)[27]. It seems as if the knees are acting as a shock absorber for the body: high frequency perturbations are partly absorbed by the knees, such that these vibrations are not transferred to the upper body.

D. Limitations & Recommendations

As measuring the full amount of 24 repetitions for all perturbation amplitudes was out of the time scope of this study, data about the cross-effects of perturbation amplitude and number of repetitions was not recorded. However, the perturbation amplitude and number of repetitions influence each other. With the limited information about the cross-effects of these two study variables, we can already hypothesize the effect of both variables combined.

A higher perturbation amplitude increases the signal-to-noise ratio and therefore decreases the noise effect on the identification result. As a result, increasing the amplitude of the perturbation can decrease the number of repetitions needed to obtain a reasonably low noise level. The other way around, increasing the number of repetitions can decrease the need for a high perturbation amplitude. This trade-off can be of use when measuring weak subjects (for example balance disorder patients), who cannot keep their balance at high perturbation amplitudes. More repetitions could be recorded for such patients, probably over the course of several trials, to preserve feasible trial lengths for these subjects.

Furthermore, in this study, 12 subjects participated. Increasing the number of subjects could increase statistical power, which might reveal more significant trends. For example, m_{NL1} seems to have a positive trend with perturbation amplitude for the low and high frequency groups as well, which might turn out to be statistically significant when more subject would be measured. The as does the SIP invalidity measure related to the hip shows a slight positive trend with amplitude, which might turn out to be significant if more subjects would be measured.

Moreover, accelerations of the support surface were used to perturb the subjects in this study. However, directly following decelerations can have a stabilizing effect without subjects having to react to the perturbation[39]. This can be a drawback of using support surface translations as a means of perturbation, which can be prevented by using manipulators that can push and pull the body[29].

The extrapolation of distortion by type I nonlinearities from the nonexcited frequencies to the excited frequencies can lead to under- and overestimates of type I nonlinearity when BLA's spectrum is not flat. The type I nonlinearity analysis can be made more robust against this problem, by using a special odd-odd multisine[36] with components at $k = 1,3,9,11,17,\dots$, however, this was not done in the present study. Use of such a perturbation signal is advised in further study of the linearity of human balance control.

The system identification technique used in this research assumes a LTI system. However, human

behaviour and motor control is time-variant[15]. This can lead to problems when averaging multiple repetitions, especially when these repetitions are recorded in different trials. Therefore, research into the time varying properties of the human balance system is advised.

Multiple input-multiple output (MIMO) system identification has already been applied to the human balance system[26,29,40]. As MIMO SI assumes a more realistic multiple inverted pendulum model, SIP assumption validity is not an issue. However, type I and type II nonlinear effects might still influence the identification result. The methods described in this paper can be adapted to be used in the analysis of MIMO SI. Furthermore, in application of MIMO SI to balance control, the methods described in this paper can give insight into possible nonlinearity of within other strategies than only the ankle strategy.

CONCLUSIONS

The goal of this study was to investigate the influence of number of repetitions and perturbation amplitude on the contributions of nonlinearity and noise to the standard deviation of BLA identification of human balance control.

Increasing the number of repetitions indeed reduces noise significantly in all three frequency groups, however, when having measured 6-8 repetitions, measuring subsequent repetitions does not decrease identification variability significantly for the subsequent 6-7 repetitions.

The balance between suppressing noise effects by using a high perturbation amplitude and minimising nonlinear effects by using a low perturbation amplitude was identified to be optimized between a perturbation signal amplitude of 8 cm PtP and 11 cm PtP. The validity of a single inverted pendulum model does not decrease significantly with perturbation amplitude.

ACKNOWLEDGEMENTS

I would like to thank Alfred Schouten, Ingrid Schut and Jantsje Pasma for their supervision and for their valuable comments that greatly improved the experiments and text of this master's thesis. Furthermore, I would like to thank the people at MotekForce Link, particularly Sanne Roeles and Frans Steenbrink, for the permission to do the experiments in Motek's showroom in Amsterdam and their instructions on operating the GRAIL system. I would like to thank Andrew Murphy for helping with the start of my graduation work while I was doing my internship in Chengdu under his supervision. Lastly, I would like to thank my family and friends for their support.

REFERENCES

1. Niam, S., Cheung, W., Sullivan, P. E., Kent, S. & Gu, X. Balance and physical impairments after stroke. *Arch. Phys. Med. Rehabil.* **80,** 1227–1233 (1999).

2. Mitchell, S. L., Collin, J. J., De Luca, C. J., Burrows, A. & Lipsitz, L. A. Open-loop and closed-loop postural control mechanisms in Parkinson's disease: increased mediolateral activity during quiet standing. *Neurosci. Lett.* **197,** 133–136 (1995).

3. Stolze, H. *et al.* Falls in frequent neurological diseases: Prevalence, risk factors and aetiology. *J. Neurol.* **251,** 79–84 (2004).

4. van der Kooij, H., van Asseldonk, E. & van der Helm, F. C. T. Comparison of different methods to identify and quantify balance control. *J. Neurosci. Methods* **145,** 175–203 (2005).

5. Engelhart, D. *et al.* Adaptation of multi-joint coordination during standing balance in healthy young and healthy old individuals. *J. Neurophysiol.* **216,** jn.00030.2015 (2015).

6. Pasma, J. H. *et al.* Reliability of System Identification Techniques to Assess Standing Balance in Healthy Elderly. *PLoS One* **11,** e0151012 (2016).

7. Boonstra, T. A., Van Vugt, J. P. P., Van Der Kooij, H. & Bloem, B. R. Balance asymmetry in Parkinson's disease and its contribution to freezing of gait. *PLoS One* **9,** (2014).

8. Boonstra, T. A., Schouten, A. C., van Vugt, J. P. P., Bloem, B. R. & van der Kooij, H. Parkinson's disease patients compensate for balance control asymmetry. *J. Neurophysiol.* **112,** 3227–39 (2014).

9. Hwang, S. *et al.* The balance recovery mechanisms against unexpected forward perturbation. *Ann. Biomed. Eng.* **37,** 1629–1637 (2009).

10. Han, K. S., Shin, S. H., Yu, C. H. & Kwon, T. K. Postural responses during the various frequencies of anteroposterior perturbation. *Biomed. Mater. Eng.* **24,** 2537–2545 (2014).

11. Runge, C. F., Shupert, C. L., Horak, F. B. & Zajac, F. E. Ankle and hip postural strategies defined by joint torques. *Gait Posture* **10,** 161–170 (1999).

12. Anderson, B. D. O. & Gevers, M. R. Identifiability of linear stochastic systems operating under linear feedback. *Automatica* **18,** 195–213 (1982).

13. Ng, T. S., Goodwin, G. C. & Anderson, B. D. O. Identifiability of MIMO linear dynamic systems operating in closed loop. *Automatica* **13,** 477–485 (1977).

14. Peterka, R. J. Sensorimotor integration in human postural control. *J. Neurophysiol.* **88,** 1097–118 (2002).

15. Peterka, R. J. & Loughlin, P. J. Dynamic regulation of sensorimotor integration in human postural control. *J. Neurophysiol.* **91,** 410–423 (2004).

16. Schieppati, M., Giordano, A. & Nardone, A. Variability in a dynamic postural task attests ample flexibility in balance control mechanisms. *Exp. Brain Res.* **144,** 200–210 (2002).

17. Mergner, T., Maurer, C. & Peterka, R. J. A multisensory posture control model of human upright stance. in *Progress in Brain Research* **142,** 189–201 (2003).

18. Park, S., Horak, F. B. & Kuo, A. D. Postural feedback responses scale with biomechanical constraints in human standing. *Exp. Brain Res.* **154,** 417–427 (2004).

19. van der Kooij, H., Donker, S., de Vrijer, M. & van der Helm, F. C. T. Identification of human balance control in standing. *Conf. Proc. - IEEE Int. Conf. Syst. Man Cybern.* **3,** 2535–2541 (2004).

20. Maurer, C., Mergner, T. & Peterka, R. J. Multisensory control of human upright stance. *Exp. Brain Res.* **171,** 231–250 (2006).

21. van Asseldonk, E. H. F. *et al.* Disentangling the contribution of the paretic and non-paretic ankle to balance control in stroke patients. *Exp. Neurol.* **201,** 441–451 (2006).

22. van der Kooij, H. & de Vlugt, E. Postural responses evoked by platform pertubations are dominated by continuous feedback. *J. Neurophysiol.* **98,** 730–43 (2007).

23. Van Ooteghem, K. *et al.* Compensatory postural adaptations during continuous, variable amplitude perturbations reveal generalized rather than sequence-specific learning. *Exp. Brain Res.* **187,** 603–611 (2008).

24. Kiemel, T., Zhang, Y. & Jeka, J. J. Identification of neural feedback for upright stance in humans: stabilization rather than sway minimization. *J. Neurosci.* **31,** 15144–53 (2011).

25. Pasma, J. H., Boonstra, T. A., Campfens, S. F., Schouten, A. C. & Van der Kooij, H. Sensory reweighting of proprioceptive information of the left and right leg during human balance control. *J. Neurophysiol.* **108,** 1138–1148 (2012).

26. Boonstra, T. A., Schouten, A. C. & van der Kooij, H. Identification of the contribution of the ankle and hip joints to multi-segmental balance control. *J. Neuroeng. Rehabil.* **10,** 23 (2013).

27. Ko, J. H., Challis, J. H. & Newell, K. M. Postural coordination patterns as a function of rhythmical dynamics of the surface of support. *Exp. Brain Res.* **226,** 183–191 (2013).

28. Jilk, J. D., Safavynia, S. A. & Ting, L. H. Contribution of vision to postural behaviors during continuous support-surface translations. *Exp. Brain Res.* **232,** 169–180 (2014).

29. Engelhart, D., Schouten, A. C., Aarts, R. G. K. M. & Van Der Kooij, H. Assessment of Multi-Joint Coordination and Adaptation in Standing Balance: A Novel Device and System Identification Technique. *IEEE Trans. Neural Syst. Rehabil. Eng.* **23,** 973–982 (2015).

30. Hwang, S., Agada, P., Kiemel, T. & Jeka, J. J. Identification of the unstable human postural control system. *Front. Syst. Neurosci.* **10,** 1–12 (2016).

31. Nashner, L. M. & McCollum, G. The organization of human postural movements: A formal basis and experimental synthesis. *Behav. Brain Sci.* **8,** 135–172 (1985).

32. Vanhoenacker, K., Dobrowiecki, T. & Schoukens, J. Design of multisine excitations to characterize the nonlinear distortions during FRF-measurements. *IEEE Trans. Instrum. Meas.* **50,** 1097–1102 (2001).

33. Winter, D. A. Biomechanics and Motor Control of Human Movement. *Processing* **2,** 277 (1990).

34. Schoukens, J., Guillaume, P. & Pintelon, R. in (ed. Godfrey, K.) 126–160 (Prentice Hall International (UK) Ltd., 1993). at <http://dl.acm.org/citation.cfm?id=167643.167650>

35. Schoukens, J., Pintelon, R. & Rolain, Y. *Mastering System Identification in 100 Exercises*. *Mastering System Identification in 100 Exercises* (2012). doi:10.1002/9781118218532

36. Schoukens, J., Pintelon, R., Rolain, Y. & Dobrowiecki, T. Frequency response function measurements in the presence of nonlinear distortions. *Automatica* **37,** 939–946 (2001).

37. Horak, F. B. & Nashner, L. M. Central programming of postural movements: adaptation to altered support-surface configurations. *J. Neurophysiol.* **55,** 1369–1381 (1986).

38. Godfrey, K. R., Tan, A. H., Barker, H. A. & Chong, B. A survey of readily accessible perturbation signals for system identification in the frequency domain. *Control Eng. Pract.* **13,** 1391–1402 (2005).

39. van Asseldonk, E. H. F., Carpenter, M. G., Van Der Helm, F. C. T. & van der Kooij, H. Use of induced acceleration to quantify the destabilizing effect of external and internal forces on posutral responses. *IEEE Trans. Biomed. Eng.* **54,** 2284–2295 (2007).

40. Pasma, J. H. *et al.* Assessing Standing Balance using MIMO Closed Loop System Identification Techniques. *IFAC-PapersOnLine* **48,** 1381–1385 (2015).

APPENDIX

A. Tables and Figures

Table 3: Group-average relative power distribution and noise-to signal ratio over excited, nonexcited odd, and nonexcited even frequencies.

	E_{ex} (%)	$E_{unex-odd}$ (%)	$E_{unex-even}$ (%)	*NSR (dB)*
Power in perturbation (position) signal: mean (SD)				
A2	99.4 (0.2)	0.4 (0.1)	0.3 (0.2)	40.3 (3.5)
A5	99.9 (0.0)	0.1 (0.0)	0.0 (0.0)	45.0 (3.7)
A8	99.9 (0.0)	0.0 (0.0)	0.0 (0.0)	47.9 (3.1)
A11	100.0 (0.0)	0.0 (0.0)	0.0 (0.0)	49.8 (3.0)
A14	100.0 (0.0)	0.0 (0.0)	0.0 (0.0)	49.7 (4.4)
A17	100.0 (0.0)	0.0 (0.0)	0.0 (0.0)	49.4 (4.0)
A20	100.0 (0.0)	0.0 (0.0)	0.0 (0.0)	50.1 (3.7)
Power in body sway signal, mean (SD)				
A2	64.8 (15.7)	8.0 (6.4)	27.2 (14.2)	-1.7
A5	88.2 (5.7)	3.8 (4.2)	8.1 (5.8)	3.2
A8	90.9 (7.1)	1.9 (1.3)	7.1 (6.8)	6.4
A11	93.6 (3.1)	1.5 (1.0)	4.9 (2.8)	8.0
A14	95.5 (2.2)	0.9 (0.5)	3.6 (1.9)	9.9
A17	96.6 (1.4)	0.8 (0.7)	2.6 (1.2)	10.6
A20	96.3 (2.3)	0.8 (0.4)	2.9 (2.2)	11.8
Power in ankle torque signal, mean (SD)				
A2	56.8 (11.7)	17.1 (6.5)	26.1 (10.4)	-0.4 (1.5)
A5	76.8 (6.8)	13.5 (5.1)	9.6 (6.6)	4.6 (3.0)
A8	82.4 (2.7)	11.0 (1.7)	6.6 (2.5)	7.5 (1.9)
A11	85.2 (2.5)	9.4 (2.2)	5.4 (2.1)	9.1 (2.1)
A14	87.1 (1.8)	8.7 (2.1)	4.3 (1.6)	11.0 (1.9)
A17	88.2 (2.5)	8.4 (2.4)	3.4 (1.0)	11.6 (1.6)
A20	89.4 (1.9)	6.9 (1.6)	3.6 (1.3)	12.3 (1.7)

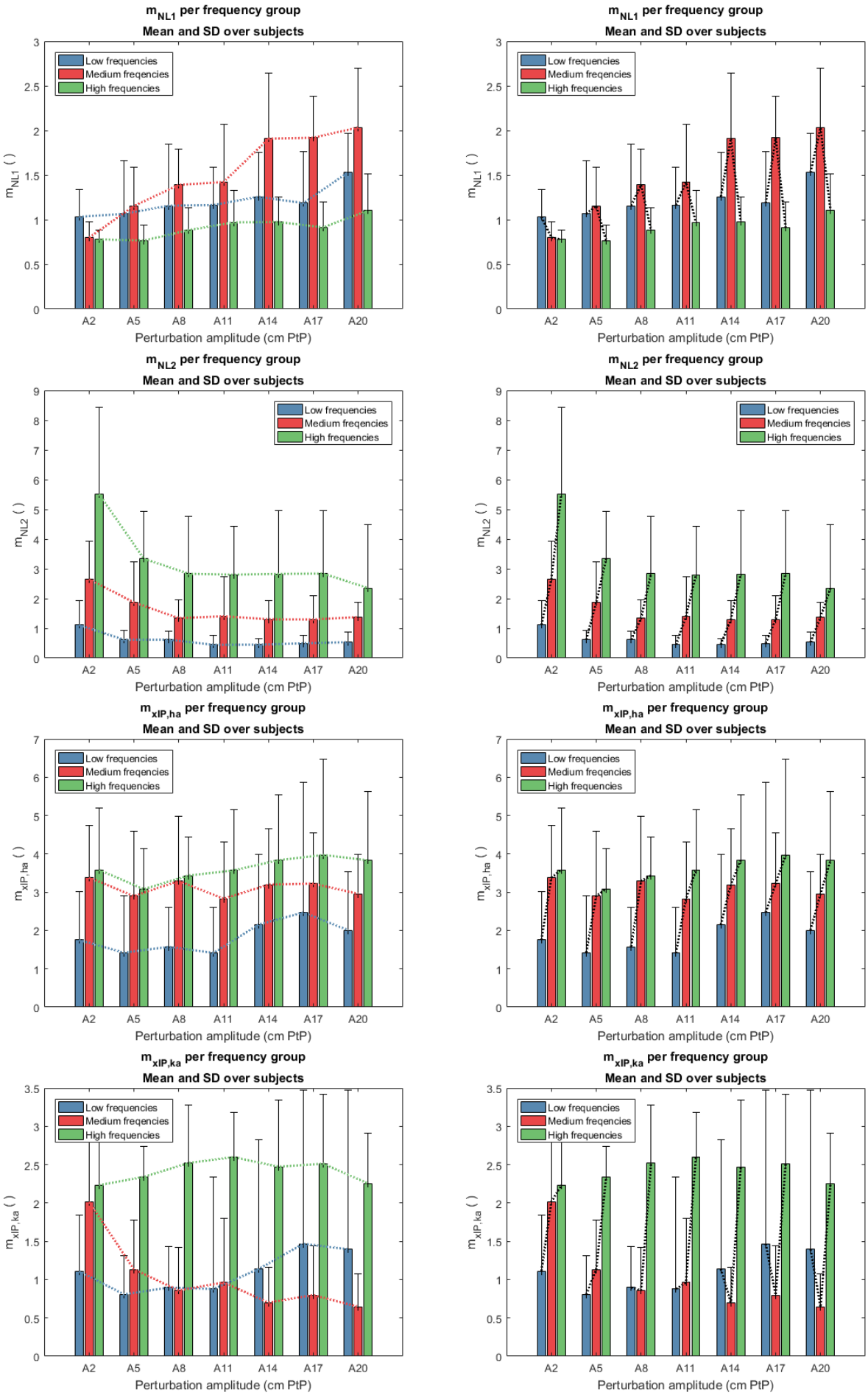

Figure 16: Four perturbation amplitude effect measures: trendlines over perturbation amplitude conditions (left) and trendlines over frequency groups (right)

Table 4: (Bonferroni corrected) p-values for pairwise comparisons of $m_{variability}$ per amount of repetitions for the low amplitude group

	R1	R2	R3	R4	R5	R6	R7	R8	R9	R10	R11	R12	R13	R14	R15	R16	R17	R18	R19	R20	R21	R22	R23
R1	x																						
R2	0.003	x																					
R3	0.002	0.818	x																				
R4	0.001	0.028	0.200	x																			
R5	0.002	0.051	0.035	1.000	x																		
R6	0.001	0.012	0.018	1.000	1.000	x																	
R7	0.003	0.242	1.000	1.000	1.000	1.000	x																
R8	0.000	0.001	0.000	0.000	0.021	0.361	1.000	x															
R9	0.000	0.002	0.000	0.000	0.004	0.784	1.000	1.000	x														
R10	0.000	0.001	0.000	0.000	0.001	0.410	1.000	1.000	1.000	x													
R11	0.001	0.002	0.000	0.000	0.000	0.275	1.000	0.730	0.424	1.000	x												
R12	0.000	0.001	0.000	0.000	0.000	0.037	1.000	0.007	0.000	0.251	0.096	x											
R13	0.000	0.001	0.000	0.000	0.000	0.056	1.000	0.016	0.003	0.000	0.003	1.000	x										
R14	0.003	0.021	0.014	0.198	0.012	1.000	1.000	1.000	1.000	1.000	1.000	1.000	1.000	x									
R15	0.001	0.002	0.001	0.001	0.004	0.131	1.000	0.319	0.032	1.000	1.000	1.000	1.000	1.000	x								
R16	0.000	0.000	0.000	0.000	0.000	0.018	0.928	0.002	0.000	0.000	0.000	0.004	0.000	1.000	1.000	x							
R17	0.000	0.001	0.000	0.000	0.000	0.017	0.742	0.003	0.000	0.000	0.000	0.004	0.001	1.000	1.000	0.462	x						
R18	0.000	0.001	0.000	0.000	0.000	0.020	0.661	0.004	0.001	0.000	0.000	0.009	0.002	1.000	1.000	0.137	1.000	x					
R19	0.000	0.000	0.000	0.000	0.000	0.013	0.475	0.002	0.000	0.000	0.000	0.002	0.001	1.000	0.498	0.010	0.118	0.321	x				
R20	0.000	0.000	0.000	0.000	0.000	0.014	0.440	0.003	0.000	0.000	0.000	0.003	0.001	1.000	0.242	0.008	0.032	0.001	1.000	x			
R21	0.000	0.000	0.000	0.000	0.000	0.010	0.340	0.002	0.000	0.000	0.000	0.002	0.000	1.000	0.069	0.003	0.008	0.000	0.011	0.001	x		
R22	0.000	0.000	0.000	0.000	0.000	0.008	0.264	0.001	0.000	0.000	0.000	0.001	0.000	0.556	0.040	0.001	0.001	0.000	0.001	0.000	0.002	x	
R23	0.000	0.000	0.000	0.000	0.000	0.007	0.201	0.001	0.000	0.000	0.000	0.001	0.000	0.302	0.014	0.001	0.001	0.000	0.000	0.000	0.000	0.003	x

No. insig.	0	3	2	4	2	8	16	5	3	4	3	3	2	9	6	2	2	1	1	0	0	0	0

Table 5: (Bonferroni corrected) p-values for pairwise comparisons of $m_{variability}$ per amount of repetitions for the medium amplitude group

	R1	R2	R3	R4	R5	R6	R7	R8	R9	R10	R11	R12	R13	R14	R15	R16	R17	R18	R19	R20	R21	R22	R23
R1	x																						
R2	0.001	x																					
R3	0.000	0.004	x																				
R4	0.000	0.001	1.000	x																			
R5	0.000	0.001	0.004	0.115	x																		
R6	0.000	0.000	0.001	0.043	1.000	x																	
R7	0.000	0.001	0.006	0.011	0.088	1.000	x																
R8	0.000	0.000	0.001	0.003	0.008	0.636	1.000	x															
R9	0.000	0.000	0.001	0.002	0.001	0.087	0.146	1.000	x														
R10	0.000	0.000	0.001	0.001	0.001	0.033	0.001	0.115	0.103	x													
R11	0.000	0.000	0.002	0.003	0.005	0.104	0.004	0.036	0.582	1.000	x												
R12	0.000	0.000	0.000	0.001	0.000	0.003	0.000	0.001	0.000	0.017	1.000	x											
R13	0.000	0.000	0.000	0.001	0.000	0.005	0.000	0.000	0.000	0.001	0.019	1.000	x										
R14	0.000	0.000	0.001	0.001	0.000	0.008	0.000	0.003	0.001	0.002	0.042	0.944	1.000	x									
R15	0.000	0.000	0.000	0.001	0.000	0.003	0.000	0.000	0.000	0.000	0.001	0.059	0.025	1.000	x								
R16	0.000	0.000	0.001	0.001	0.000	0.002	0.000	0.000	0.000	0.000	0.001	0.016	0.007	0.320	1.000	x							
R17	0.000	0.000	0.000	0.000	0.000	0.002	0.000	0.000	0.000	0.000	0.000	0.001	0.001	0.004	0.010	1.000	x						
R18	0.000	0.000	0.000	0.000	0.000	0.001	0.000	0.000	0.000	0.000	0.000	0.001	0.000	0.001	0.001	0.086	1.000	x					
R19	0.000	0.000	0.000	0.000	0.000	0.001	0.000	0.000	0.000	0.000	0.000	0.000	0.000	0.000	0.001	0.002	0.002	0.393	x				
R20	0.000	0.000	0.000	0.000	0.000	0.001	0.000	0.000	0.000	0.000	0.000	0.000	0.000	0.000	0.000	0.000	0.000	0.002	0.230	x			
R21	0.000	0.000	0.000	0.000	0.000	0.001	0.000	0.000	0.000	0.000	0.000	0.000	0.000	0.000	0.000	0.000	0.000	0.000	0.219	1.000	x		
R22	0.000	0.000	0.000	0.000	0.000	0.001	0.000	0.000	0.000	0.000	0.000	0.000	0.000	0.000	0.000	0.000	0.000	0.000	0.005	0.007	0.017	x	
R23	0.000	0.000	0.000	0.000	0.000	0.001	0.000	0.000	0.000	0.000	0.000	0.000	0.000	0.000	0.000	0.000	0.000	0.000	0.001	0.000	0.000	0.002	x
No. insig.	0	0	1	1	2	4	2	2	2	1	1	3	1	2	1	2	1	1	2	1	0	0	0

Table 6: (Bonferroni corrected) p-values for pairwise comparisons of $m_{variability}$ per amount of repetitions for the high amplitude group

	R1	R2	R3	R4	R5	R6	R7	R8	R9	R10	R11	R12	R13	R14	R15	R16	R17	R18	R19	R20	R21	R22	R23
R1	x																						
R2	1.000	x																					
R3	0.005	0.108	x																				
R4	0.003	0.007	1.000	x																			
R5	0.001	0.002	0.006	0.033	x																		
R6	0.000	0.001	0.002	0.001	1.000	x																	
R7	0.001	0.001	0.005	0.006	0.804	1.000	x																
R8	0.001	0.000	0.004	0.001	0.180	1.000	1.000	x															
R9	0.001	0.000	0.003	0.001	0.026	1.000	1.000	1.000	x														
R10	0.001	0.000	0.002	0.001	0.015	0.467	0.070	0.057	1.000	x													
R11	0.001	0.000	0.002	0.001	0.013	0.180	0.087	0.072	0.257	1.000	x												
R12	0.000	0.000	0.001	0.000	0.002	0.051	0.001	0.007	0.010	0.156	1.000	x											
R13	0.000	0.000	0.001	0.000	0.002	0.017	0.001	0.003	0.005	0.006	1.000	0.910	x										
R14	0.001	0.000	0.002	0.001	0.005	0.036	0.012	0.008	0.007	0.011	0.904	1.000	1.000	x									
R15	0.001	0.000	0.002	0.001	0.007	0.036	0.007	0.008	0.014	0.008	0.585	1.000	1.000	1.000	x								
R16	0.000	0.000	0.001	0.000	0.001	0.005	0.001	0.001	0.001	0.000	0.007	0.043	0.062	0.025	0.714	x							
R17	0.000	0.000	0.001	0.000	0.001	0.008	0.001	0.001	0.001	0.000	0.018	0.036	0.057	0.003	0.012	1.000	x						
R18	0.000	0.000	0.001	0.000	0.002	0.007	0.001	0.001	0.001	0.000	0.008	0.024	0.037	0.003	0.007	1.000	1.000	x					
R19	0.000	0.000	0.000	0.000	0.001	0.003	0.000	0.000	0.000	0.000	0.002	0.002	0.001	0.000	0.000	0.019	0.026	0.229	x				
R20	0.000	0.000	0.000	0.000	0.000	0.003	0.000	0.000	0.000	0.000	0.002	0.001	0.001	0.000	0.000	0.010	0.002	0.039	1.000	x			
R21	0.000	0.000	0.000	0.000	0.000	0.002	0.000	0.000	0.000	0.000	0.001	0.001	0.000	0.000	0.000	0.001	0.000	0.002	0.021	1.000	x		
R22	0.000	0.000	0.000	0.000	0.000	0.002	0.000	0.000	0.000	0.000	0.000	0.001	0.000	0.000	0.000	0.001	0.001	0.000	0.003	0.613	1.000	x	
R23	0.000	0.000	0.000	0.000	0.000	0.002	0.000	0.000	0.000	0.000	0.000	0.001	0.000	0.000	0.000	0.001	0.000	0.000	0.000	0.006	0.028	0.159	x
No. insig.	1	1	1	0	3	6	4	3	2	2	4	3	4	1	1	2	1	1	1	2	1	1	0

Table 7: Mean amount of insignificant p-values for the pairwise comparisons of $m_{variability}$ per amount of repetitions over all frequency groups

	R1	R2	R3	R4	R5	R6	R7	R8	R9	R10	R11	R12	R13	R14	R15	R16	R17	R18	R19	R20	R21	R22
No insig.	0.33	1.33	1.33	1.67	2.33	6	7.33	3.33	2.33	2.33	2.67	3	2.33	4	2.67	2	1.33	1	1.33	1	0.33	0.33

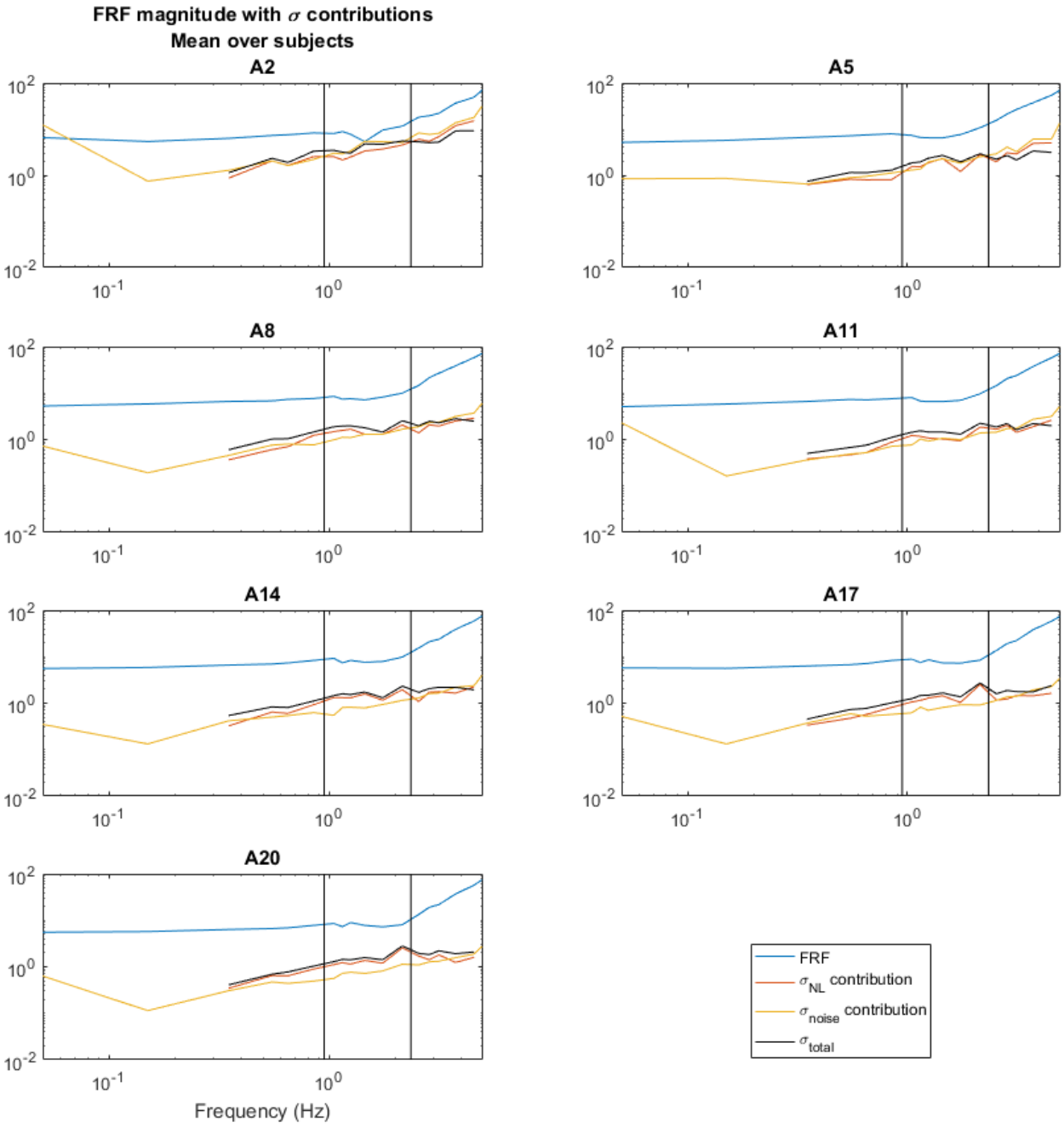

Figure 17: Mean FRF magnitude with standard deviation contributions, averaged over subjects.

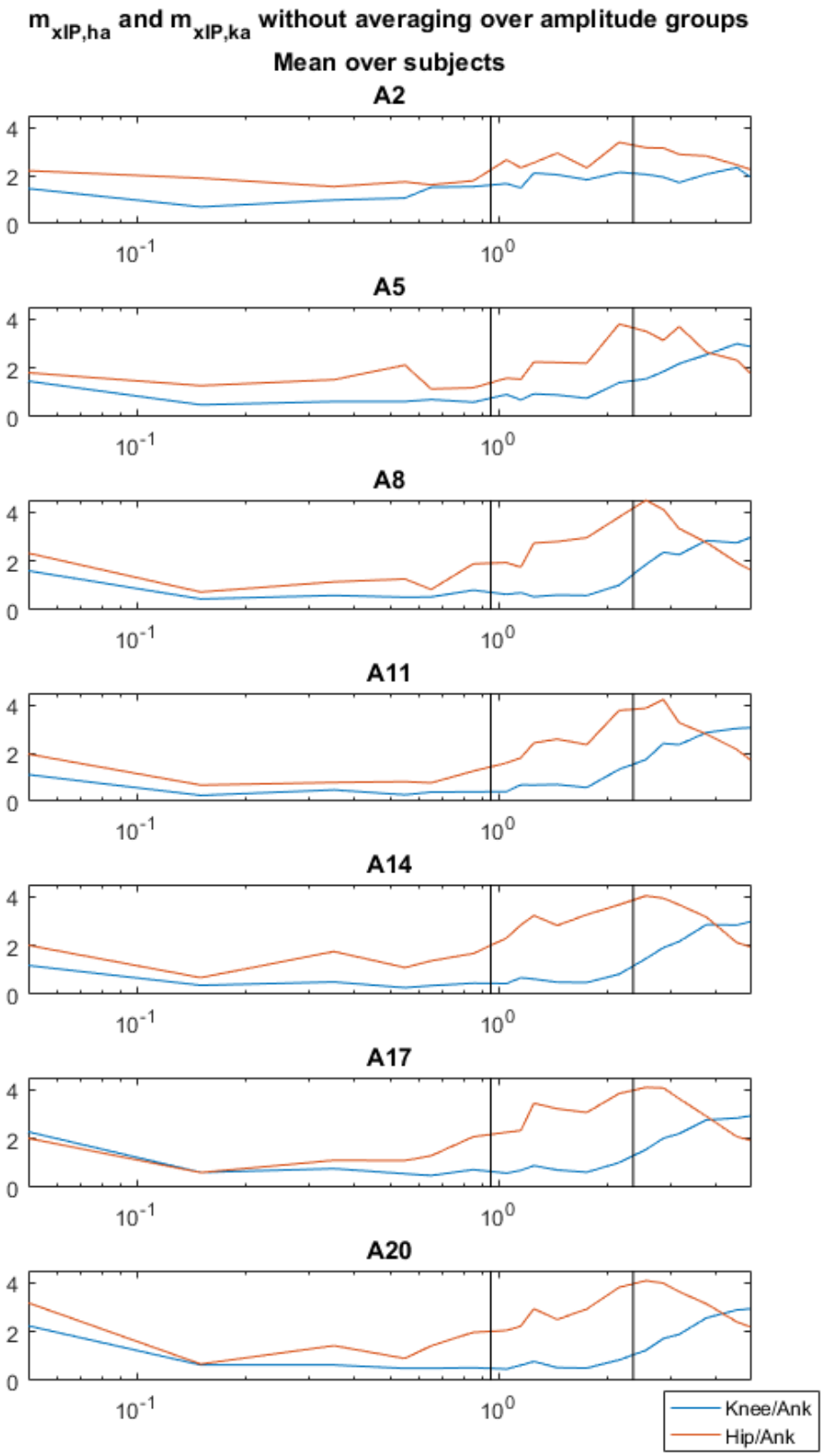

Figure 18: Mean of $m_{xIP,ha}$ and $m_{xIP,ka}$ without averaging over frequency groups, averaged over subjects

B. Human research ethics

Date 24-04-2017
Contact person Ir. J.B.J. Groot Kormelink, secretary HREC
Telephone +31 152783260
E-mail j.b.j.grootkormelink@tudelft.nl

Human Research Ethics Committee
TU Delft
(http://hrec.tudelft.nl/)

Visiting address
Jaffalaan 5 (building 31)
2628 BX Delft

Postal address
P.O. Box 5015 2600 GA Delft
The Netherlands

Ethics Approval Application: Effect of perturbation signal properties on system identification of human balance control during quite stance.
Applicant: Schouten, Alfred

Dear Alfred Schouten,

It is a pleasure to inform you that your application mentioned above has been approved.

Good luck with your research!

Sincerely,

Prof. Dr. Sabine Roeser
Chair Human Research Ethics Committee TU Delft

Prof.dr. Sabine Roeser
TU Delft
Head of the Ethics and Philosophy of Technology Section
Department of Values, Technology, and Innovation
Faculty of Technology, Policy and Management
Jaffalaan 5
2628 BX Delft
The Netherlands
+31 (0) 15 2788779
S.Roeser@tudelft.nl
www.tbm.tudelft.nl/sroeser

Figure 19: Delft University of Technology Human Research Ethics Committee approval

Delft University of Technology
ETHICS REVIEW CHECKLIST FOR HUMAN RESEARCH

This checklist should be completed for every research study that involves human participants and should be submitted before potential participants are approached to take part in your research study.

In this checklist we will ask for additional information if need be. Please attach this as an Annex to the application.

Please upload the documents (go to this page for instructions).

Thank you and please check our website for guidelines, forms, best practices, meeting dates of the HREC, etc.

I. Basic Data

Project title:	Effect of perturbation signal properties on system identification of human balance control during quite stance.
Name(s) of researcher(s):	Jurriaan de Veij Mestdagh
Research period (planning)	March 2017 – September 2017
E-mail contact person	J.C.deVeijMestdagh@student.tudelft.nl
Faculty/Dept.	3ME / BioMechanical Engineering (BMechE)
Position researcher(s):[1]	MSc student
Name of supervisor (if applicable):	Alfred Schouten
Role of supervisor (if applicable):	Associate Professor

II. Summary Research

Research question: What is the effect of perturbation signal properties on system identification of human balance control during quite stance?

Background: System identification is used to gain insight in human motor control. When using system identification on the human balance system, it can give insight in balance disorders such as stroke, Parkinson's disease and cerebral palsy and help physicians in making diagnoses, designing and evaluating rehabilitation therapy and monitoring patients. The optimal properties for the perturbation signal necessary for the system identification method are, however, unknown.

Methods: 10 to 15 healthy subjects will be placed on an instrumented treadmill (GRAIL, Motek, Amsterdam - CE certified) and will be fitted with retroreflective markers. The treadmill will move in the anterior-posterior direction according to a multisine signal. The perturbation signal properties (support surface movement amplitude) will be varied. The effect of the amplitude and the amount of repetitions on identification of the neuromuscular controller will be studied. During trails, the subject will be fitted with a safety harness. The experiments will take a total time of 1.5 hr per subject, of which approximately 50 minutes are actual trials.

[1] For example: student, PhD, post-doc

III. Checklist

	Yes	No
1. Does the study involve participants who are particularly vulnerable or unable to give informed consent? (e.g., children, people with learning difficulties, patients, people receiving counselling, people living in care or nursing homes, people recruited through self-help groups).	☐	■
2. Are the participants, outside the context of the research, in a dependent or subordinate position to the investigator (such as own children or own students)?[2]	☐	■
3. Will it be necessary for participants to take part in the study without their knowledge and consent at the time? (e.g., covert observation of people in non-public places).	☐	■
4. Will the study involve actively deceiving the participants? (e.g., will participants be deliberately falsely informed, will information be withheld from them or will they be misled in such a way that they are likely to object or show unease when debriefed about the study).	☐	■
5. Will the study involve discussion or collection of information on sensitive topics? (e.g., sexual activity, drug use, mental health).	☐	■
6. Will drugs, placebos, or other substances (e.g., drinks, foods, food or drink constituents, dietary supplements) be administered to the study participants?	☐	■
7. Will blood or tissue samples be obtained from participants?	☐	■
8. Is pain or more than mild discomfort likely to result from the study?	☐	■
9. Does the study risk causing psychological stress or anxiety or other harm or negative consequences beyond that normally encountered by the participants in their life outside research?	☐	■
10. Will financial inducement (other than reasonable expenses and compensation for time) be offered to participants?	☐	■

Important:
if your answered 'yes' to any of the questions mentioned above, please submit the full application form to HREC
(see: HREC website for forms or examples).

[2] **Important note concerning questions 1 and 2.** Some intended studies involve research subjects who are particularly vulnerable or unable to give informed consent .Research involving participants who are in a dependent or unequal relationship with the researcher or research supervisor (e.g., the researcher's or research supervisor's students or staff) may also be regarded as a vulnerable group . If your study involves such participants, it is essential that you safeguard against possible adverse consequences of this situation (e.g., allowing a student's failure to complete their participation to your satisfaction to affect your evaluation of their coursework). This can be achieved by ensuring that participants remain anonymous to the individuals concerned (e.g., you do not seek names of students taking part in your study). If such safeguards are in place, or the research does not involve other potentially vulnerable groups or individuals unable to give informed consent, it is appropriate to check the NO box for questions 1 and 2. Please describe corresponding safeguards in the summary field.

	Yes	No
11. Will the experiment collect and store videos, pictures, or other identifiable data of human subjects? [3]	☐	■
If "yes", are you sure you follow all requirements of the applicable data protection legislation? *(Please provide proof by sending us a copy of the informed consent form).*	☐	■
12. Will the experiment involve the use of devices that are not 'CE' certified?	☐	■
Only If 'yes': continue with the following questions:		
• Was the device built in-house?	☐	☐
• Was it inspected by a safety expert at TU Delft? (*Please provide device report, see: HREC website*)	☐	☐
• If it was not built in house and not CE-certified, was it inspected by some other, qualified authority in safety and approved? *(Please provide records of the inspection).*	☐	☐
13. Has or will this research be submitted to a research ethics committee other than this one? (*if so, please provide details and a scan of the approval or submission if available).*	☐	■

IV. Enclosures (tick if applicable)

- ○ Full proposal (if 'yes' to any of the questions 1 until 10)
- ○ Informed consent form (if 'yes' to question 11)
- ○ Device report (if 'yes' to question 12)
- ○ Approval other HREC-committee (if 'yes' to question 13)
- ○ Any other information which might be relevant for decision making by HREC

V. Signature(s

Signature(s) of researcher(s)
Date: 30-03-2017

Signature research supervisor (if applicable)
Date:

30-3-2017

[3] Note: you have to ensure that collected data is safeguarded physically and will not be accessible to anyone outside the study. Furthermore, the data has to be de-identified if possible and has to be destroyed after a scientifically appropriate period of time.

Appendix1: Privacy and data protection

Please fill this in if you have answered ' yes' to question 11 in the checklist

a. Are the research data made anonymous? If no, please explain.

b. Will directly identifiable data (such as name, address, telephone number, and so on) be kept longer than 6 months? If yes, will the participants give written permission to store their information for longer than 6 months?

c. Who will have access to the data which will be collected?

d. Will the participants have access to their own data? If no, please explain.

e. Will covert methods be used? *(e.g. participants are filmed without them knowing)*

f. Will any human tissue and/or biological samples be collected? *(e.g. urine)*

Figure 20: Delft University of Technology Ethics Review Checklist

Participation FIP (Feet in place) experiment

Dear participant,

Thanks for taking part in the research experiment I am performing for my graduation research thesis at Delft University of Technology. The experiment will be performed on the GRAIL (see figure), a research and rehabilitation device created by MotekForce Link. The GRAIL is located in the demo room of MotekForce Link (Hogehilweg 18C, Amsterdam) and you are expected to be there at the agreed time.

Introduction

The research is focussing on the human balance system. Therefore, in the experiment, your balance system will be provoked by having you stand on a treadmill, while the treadmill belt will move back and forth. The movement of your body will be captured using a motion capture system and force plates underneath the treadmill belt. The intent is not to tip you over, but only incite muscle reactions to the movement.

It is important to know that you can withdraw your participation at any time without any negative consequences. It is fine if you decide that you don't want to participate anymore. For me, that is also part of doing research with human subjects. Withdrawing has no negative consequences: 'no hard feelings!'.

Preparation

It's necessary to wear the supplied sports clothes (see figure) and safety harness. I will provide clothes in all sizes, so it is not necessary to bring your own sports clothes. After you have changed clothes, I will apply retroreflective markers to 8 locations on your body: on your ankles, your knees, your hips and your shoulders. These markers are part of the motion capture system, with which I capture the exact location of the markers on the computer.

After placing the markers, I will ask you to stand on the GRAIL treadmill, after which the safety harness will be secured to the ceiling.

Experiment

Now the real experiment can start. The session consists of 14 trials: we'll start with one short control trial in which you are required to stand quietly on the treadmill with your arms crossed in front of your chest. The treadmill does not move in this trial.

After the control trial, there are three practice trials of one minute, in which the treadmill belt does move. During these trials, you can get used to the movement of the treadmill belt. The trials are ordered: from a minimum belt displacement amplitude to a medium belt displacement amplitude to the maximum belt displacement amplitude. In between each trial, you can take a rest if you need it – if you don't need rest, we will just carry on with the next trial.

Finally, there are 10 trials of 2 minutes and 10 seconds, in which the treadmill belt will move with a random amplitude. This amplitude is always between the minimum and maximum amplitude that

you've already encountered in the practice trials. Between these trials, you can also take a short break if you need it.

After completing every trial, I will check the data. If all data has been recorded correctly, the experiment is done and you can change clothes again.

Please don't hesitate to ask me any questions, now or during the experiment.

Informed consent form - 2

I**nformed consent form**

Research title: Effect of perturbation signal properties on system identification of human balance control during quiet stance

Responsible researcher: Jurriaan de Veij Mestdagh

To be filled in by the participant

I confirm that I have been informed in a clear way about the nature, method, goal and [if applicable] risks and load of the experiment. I know that the data and results of the research will only be shared with third parties anonymously and confidentially. My questions are answered in a satisfactory manner. I understand that captured data or any adaptation of such will only be used for analysis and/or scientific presentations.

I agree completely voluntarily with participation in this experiment. I reserve the right to withdraw at any time without giving reasons and am informed that I will not be penalised for withdrawing nor will I be questioned on why I have withdrawn.

Participant's name: ……

Date: …… Participant's signature: ……

To be filled in by the researcher

I have explained the experiment verbally and in writing. I will answer any remaining questions about the experiment by the best of my knowledge. The participant will not be penalised for withdrawing from the experiment nor will the participant be questioned on the reason of withdrawal.

Researcher's name: ……

Date: …… Researcher's signature: ……

Informed consent form - 3

Figure 21: Informed consent form

Effect of perturbation signal properties on system identification of human balance control during quiet stance.

Research protocol

Jurriaan de Veij Mestdagh – BioMechanical Engineering (BMechE) – Delft University of Technology

Contents

1. Preparation

1.1 Materials preparation

Needed are:

- Protocol
- Informed consent
- Markers (10x)
- Double sided tape / marker tape
- Safety harnass
- Suit
- List of trials in random order
- USB stick
- Measuring tape (min 2 m)

Put 10 markers on tape

Use RandomizingTrials.xlsx, following the instructions, to get a randomized list of trials

1.2 D-flow preparation

Check D-flow configuration

Load App

If not automatically selected: enable High performance mode (pw 1234 in Amsterdam, pw 0208 in Nijmegen)

Change in filename editor (date, subject)

Open Treadmill

> Max speed 3

> Max neg speed -3

> Max acc/dec 15 m/s2

> Link belt speeds

1.3 Vicon preparation

1.3.1 Calibration

Start PC

Check sample rates of camera's (100Hz), analog channels (D-flow, 1000Hz?)

Dynamic calibration

- → Tools window – System preparation window – Calibrate Camera's – check settings ('Show Advanced)

    - Wand = Active wand
    - Calibration type = Full calibration
    - Cameras to calibrate = All cameras
    - Refinement frames = 2500
    - Wand Ratio Tolerance=0.2
    - Wand Straightness Tolerance=0.2
    - DV calibration frames = 500
    - Auto stop = yes
- → Tools window – System preparation window – Calibrate Camera's – click Start
- **ATTENTION:** Be sure to move the Active wand through the whole measurement volume of the treadmill (also at the height of the shoulders)!! Thereafter, move the Active wand through the rest of the measurement area until 2500 data points are collected for each camera.
- After calibration check:
    - Wandcount: at least 2500 for each camera
    - Image error: close to 0.1 or lower (Note that for the DV cameras the image error might be higher (if at least the image errors are 'green'). If the errors of the Vicon cameras are higher than 0.4, write this down on the measurement form. **Note that all errors should be 'green': if not, repeat the calibration!!!**

Set origin

- Change the wand mode to continuous.
- Place the metal calibration help between the treadmill belts over the special 'bump'.
- Place the wand on the metal calibration help, ensure horizontal position using the screws & check with the water level
- Start set origin: Tools window → System preparation window → Set Volume Origin → Click 'start' (start button changes into 'set origin') → click 'set origin'.

1.3.2 Check phidget or analog channel

Check whether phidget is connected and working. If it is still broken, create a new analog input as shown in the following figures.

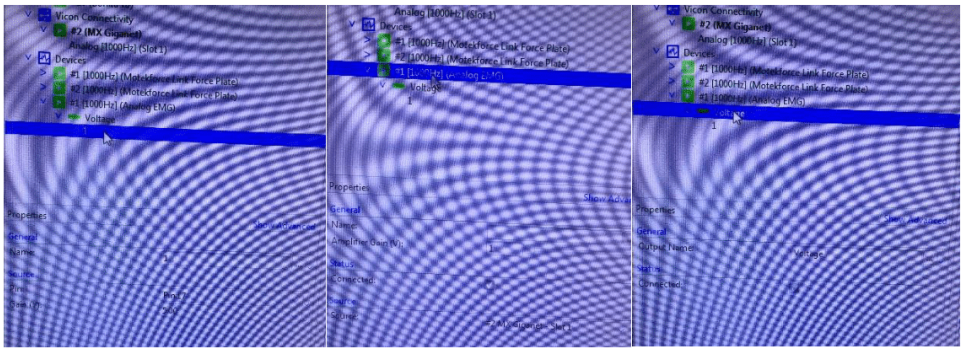

Figure 1: Creating analog input for trial cropping

1.3.3 Zero-level analog signals

Zero Nexus – zero D-flow – zero Nexus – zero D-flow

<< SUBJECT COMES IN >> **<< SUBJECT COMES IN >>**

1.3.4 Database and subject

Create new subject in Vicon database

Name: *nnnyyyymmdd* with initials and birth date

1.4 Subject preparation

1.4.1 Discuss and sign

Discuss experiment details with subject

See informed consent form

Sign informed consent form

1.4.2 Change clothes

Subject changes clothes

1.4.3 Marker placement

Markers at: LSHO, RSHO, LGT, RGT, LKNE, RKNE, LANK, RANK

Two markers on belt

Left shoulder - acromioclavicular joint
Right shoulder - acromioclavicular joint
Left trochanter major
Right trochanter major
Left knee - lateral epicondyle
Right knee - lateral epicondyle
Left ankle - lateral malleolus on an imaginary line through the transmalleolar axis
Right ankle - lateral malleolus on an imaginary line through the transmalleolar axis

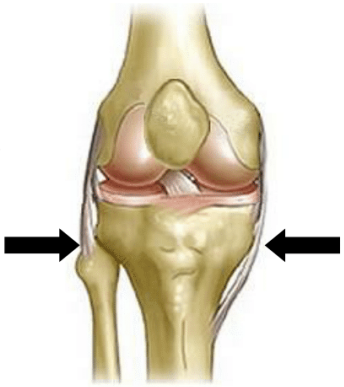

Figure 2: : Lokalization of medial and lateral epicondyl of the femur

1.4.4 Trochanter major

- *Definition:*
  The greater trochanter of the femur is located at the proximal and lateral part of the thigh, at approximately the same level as the pubic tubercle
- *Localization:*
  Stand behind the patient. Put your thumb on the posterior portion of the iliac crest with the rest of your fingers pointing downwards. Slide your fingers down untill you feel the greater trochanter.
- *Remarks:*
  To enable localisation of the greater trochanter the subject can be asked to stand on one leg while the other leg (the palpated leg) is rotated passively.

Figure 3: Localisation of major trochanter

1.4.5 Lateral femoral epicondyle

- *Definition:*
  Bony protrusion at the lateral side of the distal femur.
- *Localization:*

While the participant is standing: stand/kneel in front of the participant and instruct him/her to slightly bend the knees. Place the hands around the knee with the fingers curved around the popliteal part. Position the thumb lateral to the patella about 2 cm proximal of the joint space. Move the thumb laterally to localize the lateral epicondyle.

- *Remarks:*
  When the knee is fully extended, the iliotibial tract covers the lateral epicondyle, which makes its palpation rather difficult.
  Check whether you have marked the correct position by having the participant make several knee bends. The marked position should not move mediolaterally or anteroposteriorly relative to the femur (i.e. the point of rotation of the knee).

1.4.6 Lateral malleolus

- *Definition:*
  Bone protrusion at the lateral side of the distal tibia.
- *Localization:*
  Determine the center of the bone protrusion at the lateral side of the ankle.
- *Remarks:*
  By positioning your fingers around the lateral malleolus, you can determine the center of the malleolus.

1. Leg length: distance between ASIS and medial malleolus
   Measure with tape measure
   When the subject is able to stand up straight, you can measure the leg length in two steps: 1) the distance from ASIS to medial femoral epicondyle and 2) the distance from medial epicondyle to medial malleolus. The combined lengths give the leg length.

Marker placement

a) Try to minimize the presence of fabric to be able to attach markers to the skin itself
b) **Marker locations**: see above
c) Use double-sided tape to attach the markers to the body. Prepare the markers in advance when possible to minimize preparation time
d) Pay careful attention to the exact placement of the makers. Try to locate the anatomical landmarks (8.1) with care and be sure to have the same way of location/placement for all subjects over the whole project.
e) For markers which are more prone to become detached during the experiment use additional tape to attach the marker base to the body
f) Try to minimize contact with the reflective surface of the makers as this will reduce the reflective capabilities in time. Try to handle the markers on the base.

1.4.7 Subject length measurement

Measure subject's length

2. Feet-in-place test

2.1 Explanation

We will perform the Feet-in-place test on the treadmill. First the participant will get familiar with the task by standing as normal as possible for 20 seconds with their feet placed against the lines and their arms crossed against their chest. During the real experiment, this task will be performed ten times for 130 seconds. Conditions (A2 - A5- A8 - A8_2 - A8_3 – A8_4 – A11 – A14 – A17 – A20) are presented in a random order.

2.2 Preparation

2.2.1 D-flow

- Open the FIP application:
  - USB:\D-Flow app\yyyy-mm-dd\yyyymmdd_adaptedJurriaan.dflow
  - Click 'Yes'
  - Code: 0208 (N) / 1234 (Ams) → OK
- Zero level forceplates

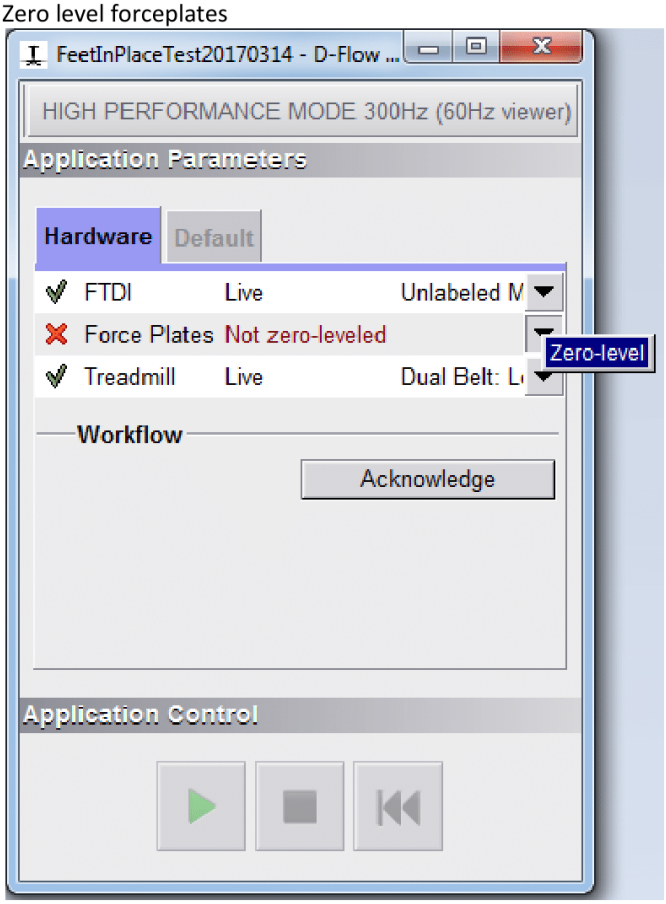

- Click 'Acknowledge'
- Make the runtime console window wider
- Open Filename editor window: View → Filename Editor (F7)

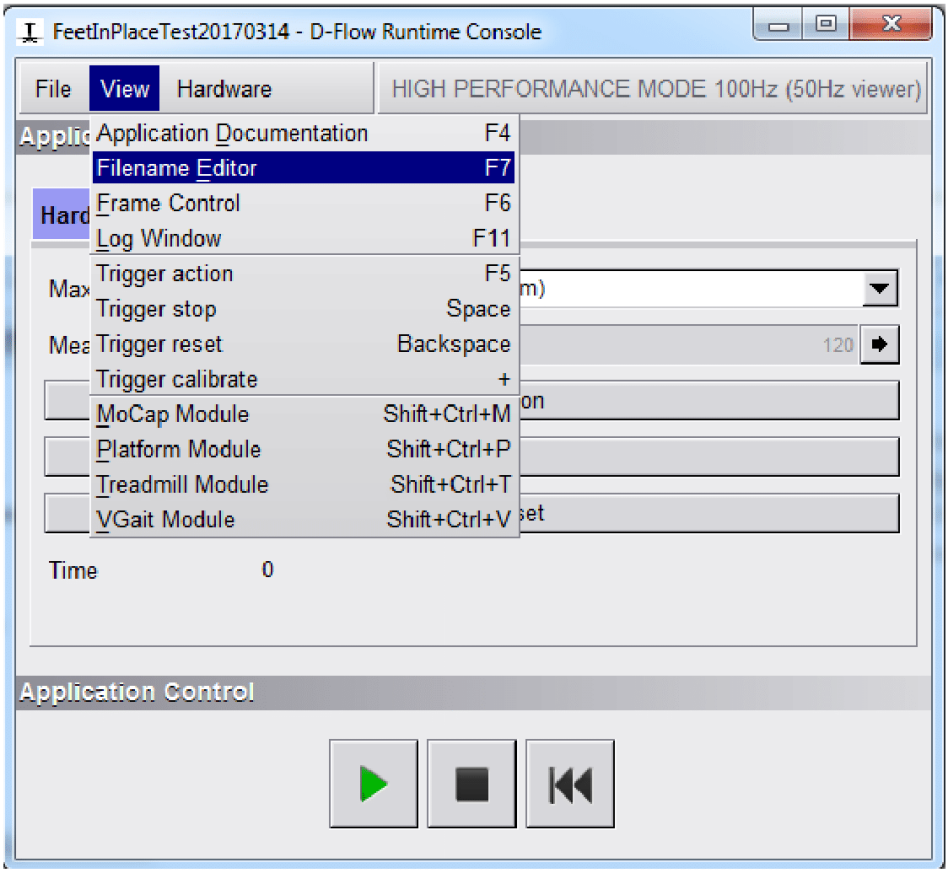

-
- Save data:
    - Click on button next to 'Record' ()
    - %DATA%\Jurriaan→ New Folder *"yyyymmdd"* (date of test) → New Folder *"nnnyyyymmdd"* (subject identifier)
    - Name trial: nnnyyyymmdd_*roundx_Axx*
    - ExamplePath (familiarization round) = %DATA%\Jurriaan\20170418\mjm19900426\mjm19900426_round1_F08.csv
    - ExamplePath (16 cm ptp round) = %DATA%\Jurriaan\20170418\mjm19900426\mjm19900426_round1_A16.csv
    - Close Filename Editor window

2.3 Experiment Practice (practice trial)

2.3.1 Vicon

- Tools window – Capture window – Next Trial Setup →
    - **Trial name Vicon: nnnyyyyddmm_roundx_Fxx**
    - Select "Auto increment trial number"
- Tools window – Capture window – Open Data Source set up →
    - Select data: MX camera data; DV camera data; Analog Data
- Tools window – Capture window – Open Data Source set up →
    - Select: "Stop duration after 30 seconds"

2.3.2 D-flow

- Runtime console
    - Measurement time: Familiarisation – 60s
- Click 'Show Position' to show the projection lines on the belt → Make sure participant is standing correctly
- Click 'Start' to start the perturbation
- Click 'Stop en Reset' when the trial is finished

2.3.3 General

- Instruction for the participant:
    - First we will first get familiar with this trial
    - Stand with the feet against the lines.
    - Try to stand relaxed, as normal as possible.
    - Keep the knees extended (no hyperextension!) and look straight forward.
    - Keep your arms crossed against your chest.
    - Instruct the participant that the treadmill will move several centimeters backwards and forwards.

- Note the following:
    - Success or failure (foot lift/ foot shift / step = failure). When failure, try the trial again. When failure again, move on to the next trial.
    - Remarks: any other observations

2.4 Data Check

- Check whether the data was recorded correctly in 1 trial
    - Vicon
        - Marker data (Reconstruct)
        - Force plate data (check voltages of sensors (should be between -1 and +1)!!)
        - Videos
    - D-flow (C:/CAREN Resources/Data/MoveOn/*Subjectcode*/FIP/…)
        - Amplitude
        - Forces

2.5 Static trial (initialization)

2.5.1 Recording

Filename: nnnyyyymmdd_roundx_S

Record 20 seconds of static quiet standing in Vicon.

2.5.2 Labeling

Check markers & analog: **QUALITY CHECK → 100%?**

Label subject using template *IMDI-FeetInPlaceTest.vst*

2.5.3 Saving subject

Save initialization subject

2.6 Experiment Real

2.6.1 D-flow

- Measurement time: 120 (s)
- Click 'Show Position' to show the projection lines on the belt → Make sure participant is standing correctly
- Click 'Start' to start the perturbation
- Click 'Stop en Reset' when the trial is finished

2.6.2 General

- Instruction for the participant:
    - Now we start with the real experiment. Ten tests of 2 minutes, with breaks in between of 1 minute minimum.
    - Stand with the feet against the lines.
    - Try to stand relaxed, as normal as possible.
    - Keep the knees extended (no hyperextension!) and look straight forward.
    - Keep your arms crossed against your chest.
    - Instruct the participant that the treadmill will move several centimeters backwards and forwards.

- Note the following:
    - Success or failure (foot lift/ foot shift / step = failure). When failure, try the trial again. When failure again, move on to the next trial.
    - Remarks: any other observations

2.7 Finalizing

- The participant should step off the treadmill after the static balance test has been finished.
- Check whether all data was recorded

3. After the experiment

3.1 D-flow

Close app (don't save)

Copy all data from C:\CAREN Resources\Data to USB:\D-Flow data\

3.2 Vicon

Reconstruct using 'grey bubbles button'

Use labeling skeleton "FIP_DVM"/"JurriaanFIP"

Autolabel if possible

Label markers as follows:

- rsho – lsho (shoulder)
- rgt – lgt (greater trochanter – hip)
- rkne – lkne (knee)
- rank – lank (ankle)
- rtrm – ltrm (treadmill)

Fill holes if necessary:

1. Woltring ≤ 20 frames
2. More complex > 20 frames

Check quality in quality tab

Check analog channels

Switch USB to MoCap computer

Copy all data files from Vicon database into USB:\Vicon

Figure 22: Research protocol

Effect of perturbation signal properties on system identification of human balance control during quiet stance.

SUBJECT: **(nnnyyyymmdd)**

DATE OF TODAY: **(yyyymmdd)**

Preparation

- ☐ All materials
- ☐ Checked D-flow config (High performance mode 1234A 0502T, max speeds etc)
- ☐ Calibrated Vicon Nexus
- ☐ Phidget or analog channel
- ☐ Zero level Nexus – D-flow – Nexus – D-flow

Subject comes in

Subject

- ☐ Discuss experiment details with subject
- ☐ Sign forms
- ☐ Created new subject in Vicon nnnyyyymmdd (birth date)
  - Folder in subject: yyyy-mm-dd round x (todays date)
- ☐ Subject changes clothes
- ☐ Markers placed at
  - Shoulders
  - Hips
  - Knees
  - Ankles
  - Treadmill
- ☐ Measured subject length

FIP

- ☐ Zero level forceplates
- ☐ Changed D-flow filenames
- ☐ Static measurement
  - Checked data
- ☐ Instruction: arms crossed, relaxed, quiet stance
- ☐ 3 x familiarisation trial
  - While: excel randomization

COND	A__	A__	A__	A__	A__	A__	A__	A__	A__	A__
NAMECHANGE										
CHECK DATA										

- ☐ Instruction again
- ☐ Amplitude conditions
  - Changes names: nnnyyyymmdd_roundx_Ax
- ☐ Checked all data

Figure 23: Research protocol checklist.